Modeling the effects of hydrology on ecosystem respiration at Mer Bleue bog

Dimitre D. Dimitrov,[1] Robert F. Grant,[2] Peter M. Lafleur,[3] and Elyn R. Humphreys[4]

Received 16 February 2010; revised 7 September 2010; accepted 10 September 2010; published 31 December 2010.

[1] The *ecosys* model was applied to examine the effects of peatland hydrology on soil respiration and ecosystem respiration at Mer Bleue peatland, Ontario, Canada. It was hypothesized that a decrease in near-surface microbial respiration in peat hummocks resulting from water table (WT) drawdown and subsequent desiccation of the uppermost peat would offset an increase of soil respiration at depth with improved aeration (respiration offsetting mechanism). In contrast, shallower water table in hollows would not allow near-surface desiccation to offset increased soil respiration at depth during drying. However, increased hollow soil respiration with WT drawdown would be offset by decreased aboveground moss respiration with near-surface desiccation in hummocks. Model results for microbial respiration were tested against independent laboratory experiments and ecosystem respiration against hourly eddy-covariance measurements of bog CO_2 exchange from 2000 to 2004. The respiration offsetting mechanism modeled in hummocks resulted in CO_2 production of 0.85 μmol CO_2 m^{-2} s^{-1} with both low (67 cm) and intermediate (38 cm) water tables in the summers of 2001 and 2004, and of 0.81 μmol CO_2 m^{-2} s^{-1} and 0.95 μmol CO_2 m^{-2} s^{-1} with high (31 cm) and intermediate (41 cm) water tables in the summers of 2000 and 2001. Ecosystem respiration was 2.01 μmol CO_2 m^{-2} s^{-1} and 2.23 μmol CO_2 m^{-2} s^{-1}, and 2.62 μmol CO_2 m^{-2} s^{-1} and 2.58 μmol CO_2 m^{-2} s^{-1}, respectively, during these periods. Our results suggest that ecosystem respiration at Mer Bleue varied little with water table, but this behavior may not be typical for other peatlands.

Citation: Dimitrov, D. D., R. F. Grant, P. M. Lafleur, and E. R. Humphreys (2010), Modeling the effects of hydrology on ecosystem respiration at Mer Bleue bog, *J. Geophys. Res.*, *115*, G04043, doi:10.1029/2010JG001312.

1. Introduction

[2] Carbon stored in peatlands is estimated to be between 200 and 450 Pg [*Roulet et al.*, 2007; *Gorham*, 1991] and accounts roughly for one third of the world's soil carbon pool. Therefore, ecological controls on peatland carbon balance are of great interest. Particularly, the water balance of peatlands has long been considered a key control for all the physical, chemical and biological processes in peat [*Lafleur et al.*, 2003, 1997; *Shurpali et al.*, 1995]. However, the overall influence of soil water on ecosystem respiration (ER) in peatlands has been questioned recently [*Lafleur et al.*, 2005a] as various, sometimes contradictory observations have been reported in the literature. The ER response to varying water table (WT) depths is further complicated by covariation of water table with soil temperatures [*Lafleur et al.*, 2005a]. Therefore, a key question in peatland research is "how vulnerable is peatland carbon, to changes in peat water contents (θ) and water table"?

1.1. Effects of Peat Water Content θ on CO_2 Production

[3] Field chamber measurements, as well as in situ and laboratory incubations, both support [*Sulman et al.*, 2009; *Strack and Waddington*, 2007; *Bubier et al.*, 2003a, 2003b; *Oechel et al.*, 1998; *Silvola et al.*, 1996a] and refute [*Strack and Waddington*, 2007; *Updegraff et al.*, 2001; *Bubier et al.*, 1998; *Bridgham et al.*, 1991] the dependence of ecosystem respiration on WT fluctuations. Some studies suggest that soil respiration in peat profiles increases with increased drying and aeration at depth [*Moore and Dalva*, 1993]. Others claim that CO_2 production rates decrease as θ deviates above or below an optimum value [*Silvola and Ahlholm*, 1989]. This optimum value was found to vary from ~0.6 m^3 m^{-3} estimated by modeling [*Frolking et al.*, 2002] to ~0.9 m^3 m^{-3} determined experimentally [*Waddington et al.*, 2001]. Although

[1]Northern Forestry Centre, Canadian Forest Service, Edmonton, Alberta, Canada.
[2]Department of Renewable Resources, University of Alberta, Edmonton, Alberta, Canada.
[3]Geography Department, Trent University, Peterborough, Ontario, Canada.
[4]Department of Geography and Environmental Studies, Carleton University, Ottawa, Ontario, Canada.

0148-0227/10/2010JG001312

the latter number seems high, it is consistent with *Orchard et al.* [1992], who suggested that stimulating effects of increasing θ selectively allows various microbial communities to become active under different moisture conditions. *Silvola et al.* [1996a] found that initial WT decline from peat surface resulted in a pronounced increase of CO_2 emission, which became less pronounced with further WT decline down to ~30 cm depth, and even slightly decreased with water table dropping below ~30–40 cm. *Sulman et al.* [2009] found that the initial WT drawdown caused an increase of CO_2 emission, which became less pronounced with WT decline below ~25–30 cm depth.

[4] *Strack and Waddington* [2007] reported increased respiration in hollows but no significantly different respiration in hummocks with lowereing of the water table. Their study was one of the few that considered peatland microtopography and treated separately respiration in hummocks from respiration in hollows. Other recent field experiments have reported a lack of correlation between the WT depth and ecosystem respiration [*Lafleur et al.*, 2005a; *Moore et al.*, 2003; *Updegraff et al.*, 2001; *Scanlon and Moore*, 2000], mostly explained by the small contribution of deep peat [*Blodau et al.*, 2007]. Limited CO_2 production from deep peat was attributed to (1) the low proportion of readily available organic carbon [*Updegraff et al.*, 1995; *Nadelhoffer et al.*, 1991], (2) accumulation of recalcitrant humic compounds [*Hogg et al.*, 1992], (3) unavailability of suitable electron acceptors [*Lafleur et al.*, 2005a; *Frolking et al.*, 2001; *Waddington et al.*, 2001], and (4) low soil temperatures at depth [*Blodau et al.*, 2007].

1.2. Advances in Modeling of Hydrological Effects on Respiration

[5] Process-based models are well suited for investigating the effects of hydrology on ecosystem respiration because it is possible to distinguish the effects of moisture from those of soil temperature and nutrients within the peat profile. The *ecosys* model [*Grant*, 2001], which couples ecosystem hydrology, soil thermal regime and carbon balance, has been shown to simulate reasonably well hourly dynamics of water table, θ and soil temperatures at various depths in hummocks and hollows [*Dimitrov et al.*, 2010a, 2010b]. The model was applied to simulate bog ecosystem respiration in this study.

[6] *Ecosys* has an advantage to other models for peat carbon balance, such as PCARS [*Frolking et al.*, 2002], PDM [*Frolking et al.*, 2001], InTEC V3.0 [*Ju et al.*, 2006] and MWM [*St-Hilaire et al.*, 2008], in that it can explicitly simulate CO_2 production in soil by diverse heterotrophic and autotrophic microbial populations that drive substrate hydrolysis, oxidation-reduction reactions and nutrient uptake, which in turn drive microbial growth [*Grant*, 2001]. Oxidation-reduction reactions in *ecosys* are determined by demand for and supply of electron acceptors, such as O_2, NO_3^-, NO_2^-, N_2O, H_2, and reduced C [*Grant and Pattey*, 2003, 1999; *Grant and Roulet*, 2002; *Grant and Rochette*, 1994], so that a range of aerobic and anaerobic reactions are simulated. In contrast, most of the above peatland models simulate decomposition and respiration by prescribed first-order decay rates as hydrological effects on these processes are formulated through empirical multipliers.

1.3. Objectives and Hypotheses

[7] The main objective of this research is to understand and model the effects of subsurface hydrology on soil respiration in bog hummocks and hollows, and on bog ecosystem respiration. A secondary objective is to explain and reconcile the contrasting effects of water table on ecosystem respiration observed in peatlands, as summarized above, through modeling the effects of subsurface peat hydrology, and fibric peat thickness and high macroporosity, on microbial and root respiration.

1.3.1. Soil Respiration in Hummocks

[8] It has been shown previously that water table drawdown in *ecosys* model creates desiccation in the near-surface peat in hummocks [*Dimitrov et al.*, 2010a, 2010b; *Dimitrov*, 2009], which was consistent with field observations of rapid drainage through the high macropore fraction of the fibric peat (Figure 1) [*Lafleur et al.*, 2005a; *Silins and Rothwell*, 1998]. In this study we hypothesize that in hummocks decrease of near-surface microbial respiration through reducing microbial habitat with near-surface drying would be offset by the increase of microbial and root respiration at depth with water table drawdowns and improved aeration. Hereafter, this response is referred as a respiration offsetting mechanism in hummocks and is addressed by *ecosys* as follows. Increase of aqueous concentration of active microbial biomass with desiccation in the model results in microbial competitive inhibition [*Grant*, 2001; *Lizama and Suzuki*, 1991], which slows substrate decomposition (hydrolysis), thus reducing uptake of decomposition products by microbes in the most productive near-surface peat. Slower uptake decreases the active microbial biomass at near-surface, further slowing decomposition and thus promoting low respiration rates. As water table recedes, gaseous O_2 diffusion increases at depth, which results in increased aqueous O_2 concentrations, and shift from anaerobic to aerobic microbial respiration in above water table. The transition from anaerobic to aerobic respiration results in higher energy yield, increasing microbial biomass growth, hence respiration. Vascular root respiration and moss rhizoid respiration also increase with increased root O_2 uptake and increased root growth and densities, and a larger respiring root biomass.

1.3.2. Soil Respiration in Hollows

[9] We hypothesize that in hollows lack of near-surface desiccation [*Dimitrov et al.*, 2010a, 2010b; *Dimitrov*, 2009] due to the thin fibric peat (Figure 1), together with improved aeration at depth would result in increased respiration with water table drawdown. However, this increase would be less than that in hummocks due to the waterlogged deep peat with predominating anaerobic respiration.

1.3.3. Aboveground Plant Respiration

[10] Shrubs would compensate for the near-surface drying through their deeper roots, thus maintaining conservative shrub water potential, productivity and aboveground respiration. However, a decrease in aboveground moss respiration in hummocks with declining moss water potential and productivity caused by the near-surface drying would largely offset increased hollow soil respiration.

1.3.4. Ecosystem Respiration

[11] As described above, increase of deep peat respiration with water table drawdown would be offset by concurrent decreases of near-surface soil respiration and aboveground

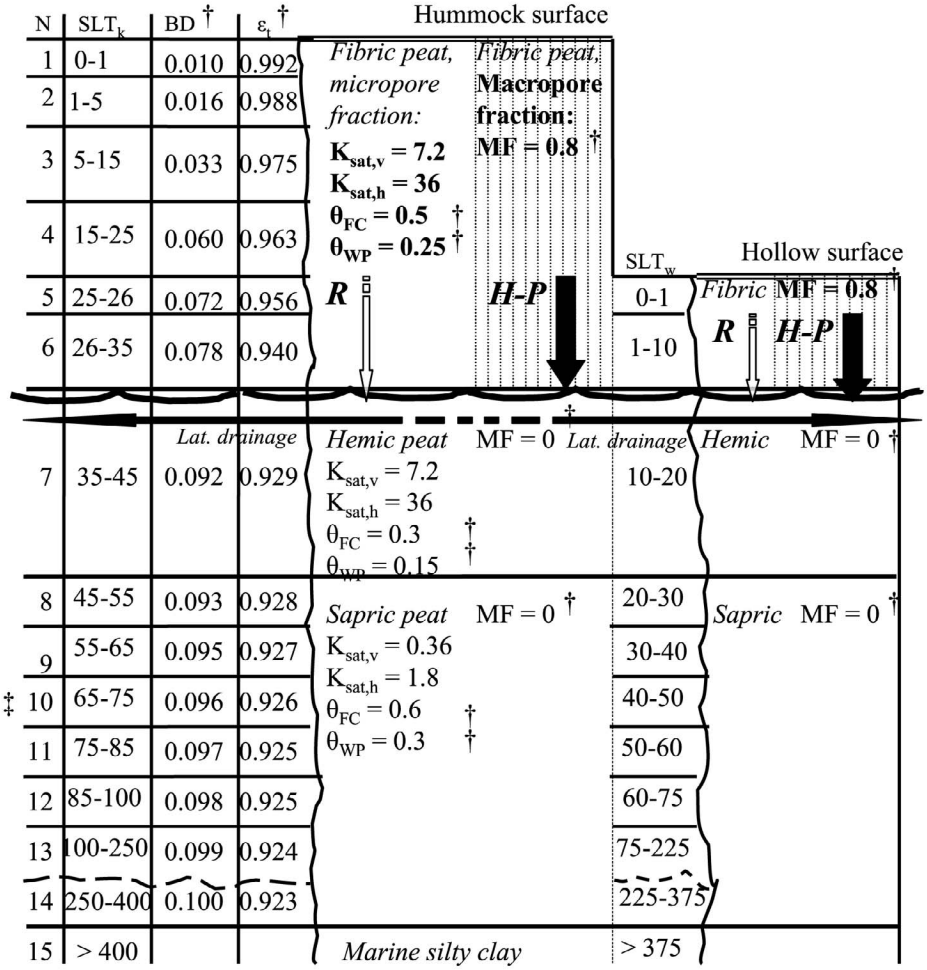

† peat parameters measured and derived for Mer Bleue bog
‡ soil layer with max. water table depth of 70 cm below the hummock surface

Figure 1. Graphical scheme of the peat profile at Mer Bleue bog. H-P is the Hagen-Poiseuille flow through the volumetric macropore fraction MF ($m^3\ m^{-3}$) of the fibric peat, i.e., MF = 0.8 $m^3\ m^{-3}$; R is the Richards flow through the peat micropore (matrix) fraction of fibric peat, and through hemic and sapric peat with no macroporosities, i.e., MF = 0 $m^3\ m^{-3}$ [*Dimitrov*, 2009; *Schwarzel et al.*, 2002]; N is the number of soil layers, starting from the hummock surface; SLT_k (cm) and SLT_w (cm) are the soil layer depths from the hummock and hollow surfaces; BD (Mg m^{-3}) is the bulk density of peat with macropores, for layers 1–10 [*Blodau and Moore*, 2002] and 11–15 [*Frolking et al.*, 2002, 2001]; ε_t ($m^3\ m^{-3}$) is the soil layer total porosity, calculated from the corresponding BD; $K_{sat,v}$ (mm h^{-1}) is vertical saturated hydraulic conductivity for peat matrix [*Letts et al.*, 2000]; $K_{sat,h}$ (mm h^{-1}) is horizontal saturated hydraulic conductivity for peat matrix, assumed to be five times $K_{sat,v}$ [*Reeve et al.*, 2000]; θ_{FC} ($m^3\ m^{-3}$) is water content at field capacity, and θ_{WP} ($m^3\ m^{-3}$) is water content at wilting point for peat matrix (N. Roulet, personal communication, 2005).

plant respiration on hummocks, thus resulting in ecosystem respiration that is relatively unaffected by variations of water table.

2. Model Development

[12] *Ecosys* equations for soil hydrology are originally described by *Grant* [2001] and summarized for peat by *Dimitrov et al.* [2010a, 2010b]. Relevant *ecosys* equations for microbial hydrolysis, respiration and growth, autotrophic belowground respiration and growth, aboveground respiration, and O_2 transport and transfer through the soil and the plants [*Grant*, 2004, 2001, 1998a, 1998b, 1993, 1989; *Grant and Roulet*, 2002; *Grant and Rochette*, 1994; *Grant et al.*, 2007, 2004, 1993a, 1993b], are given in Appendices A–E. Equation parameters are especially described with their values and literature sources in Table 1, and equation variables and indexes are given in the notation section.

Table 1. Parameters in *Ecosys* Equations of Appendices A–E

Term	Definition	Unit	Value	Relevant Equation	Reference
$D_{Sj,B}$	Specific decomposition rate of $B_{i,j,C}$ by $\sum_n M_{i,n,a}$ at 25°C, saturating substrate [$S_{i,C}$], N, P contents, i = sorbed organic matter, j = sorbed organic matter	[g C g MC^{-1} h^{-1}]	0.1875	(A1b)	*Grant et al.* [2007]
$D_{Mhi,n,l}$	Specific decomposition rate of $M_{i,n,j}$ at 30°C *(X = hi,n; j = l)*	[g C g MC^{-1} h^{-1}]	0.0125	(A16)	*Grant et al.* [1993a, 1993b]
$D_{Mhi,n,r}$	Specific decomposition rate of $M_{i,n,j}$ at 30°C *(X = hi,n; j = r)*	[g C g MC^{-1} h^{-1}]	0.00035	(A16)	*Grant et al.* [1993a, 1993b]
$D_{Sj,C}$	Specific decomposition rate of $S_{i,j,C}$ by $\sum_n M_{i,n,a}$ at 25°C, saturating substrate [$S_{i,C}$], N, P contents, i = (woody and fine litter, manure) j = protein	[g C g MC^{-1} h^{-1}]	0.75	(A1a)	*Grant et al.* [2007]
	Specific decomposition rate of $S_{i,j,C}$ by $\sum_n M_{i,n,a}$ at 25°C, saturating substrate [$S_{i,C}$], N, P contents, i = (woody and fine litter, manure) j = carbohydr.	[g C g MC^{-1} h^{-1}]	0.75	(A1a)	*Grant et al.* [2007]
	Specific decomposition rate of $S_{i,j,C}$ by $\sum_n M_{i,n,a}$ at 25°C, saturating substrate [$S_{i,C}$], N, P contents, i = (woody and fine litter, manure) j = cellulose	[g C g MC^{-1} h^{-1}]	0.1125	(A1a)	*Grant et al.* [2007]
	Specific decomposition rate of $S_{i,j,C}$ by $\sum_n M_{i,n,a}$ at 25°C, saturating substrate [$S_{i,C}$], N, P contents i = (woody and fine litter, manure) j = lignin	[g C g MC^{-1} h^{-1}]	0.01875	(A1a)	*Grant et al.* [2007]
	Specific decomposition rate of $S_{i,j,C}$ by $\sum_n M_{i,n,a}$ at 30°C, saturating substrate [$S_{i,C}$], N, P contents, i = (POM) j = POM	[g C g MC^{-1} h^{-1}]	0.025	(A1a)	*Grant et al.* [1993a, 1993b]
	Specific decomposition rate of $S_{i,j,C}$ by $\sum_n M_{i,n,a}$ at 30°C, saturating substrate [$S_{i,C}$], N, P contents, i = (humus) j = humus	[g C g MC^{-1} h^{-1}]	0.005	(A1a)	*Grant et al.* [1993a, 1993b]
$D_{Zj,C}$	Specific decomposition rate of $Z_{i,j,C}$ by $\sum_n M_{i,n,a}$ at 25°C, saturating substrate [$S_{i,C}$], N, P contents, i = (litter, manure, POM, humus) j = labile	[g C g MC^{-1} h^{-1}]	0.1875	(A1c)	*Grant et al.* [2007]
	Specific decomposition rate of $Z_{i,j,C}$ by $\sum_n M_{i,n,a}$ at 25°C, saturating substrate [$S_{i,C}$], N, P contents, i = (litter, manure, POM, humus) j = resistant	[g C g MC^{-1} h^{-1}]	0.0375	(A1c)	*Grant et al.* [2007]
E_m	Energy requirement for growth of $M_{i,n,a}$	[kJ g C^{-1}]	25	(A6), (A8), (A10a), (A12)	*McGill et al.* [1981]
F_l	Fraction of microbial growth allocated to the labile component $M_{i,n,l}$	[-]	0.55	(A18)	*Grant et al.* [1993a, 1993b]
F_r	Fraction of microbial growth allocated to the resistant component $M_{i,n,r}$	[-]	0.45	(A18)	*Grant et al.* [1993a, 1993b]
$\Delta G'_f$	Free energy yield of fermentation and acetogenesis *(n = f)*	[kJ g C^{-1}]	−4.43	(A10b)	*Brock and Madigan* [1991]
$\Delta G'_m$	Free energy yield of acetotrophic methanogenesis *(n = m)*	[kJ g C^{-1}]	−1.03	(A12)	*Brock and Madigan* [1991]
$\Delta G'_{O2}$	Free energy yield of aerobic oxidation *(n = e, n ≠ d, t)*	[kJ g C^{-1}]	−37.5	(A6)	*Brock and Madigan* [1991]
$\Delta G'_{O2,d}$	Free energy yield of denitrifier aerobic oxidation *(n = d)*	[kJ g C^{-1}]	−25	(A6)	*Koike and Hattori* [1975]
K_D	Michaelis-Menten constant for hydrolysis	[g C g MC^{-1}]	75	(A1a)–(A1c)	*Lizama and Suzuki* [1991]
K_{QC}	Michaelis-Menten constant for $R_{hi,e}$ on [$Q_{i,c}$]	[g C m^{-3}]	36	(A3), (A4)	*Grant et al.* [2007]
K_{O2}	Michaelis-Menten constant for O_2 reduction	[g O m^{-3}]	0.032	(A5a), (B5a)	*Griffin* [1972]
K_f	Michaelis-Menten constant for fermentation and acetogenesis	[g C m^{-3}]	36	(A9)	*McGill et al.* [1981]
K_m	Michaelis-Menten constant for $A_{i,c}$ uptake by ac. methanogens	[g C m^{-3}]	12	(A11)	*Zehnder et al.* [1980]
K_{iD}	Inhibition constant for hydrolysis	[g C g MC^{-1}]	25	(A1a)–(A1c)	*Lizama and Suzuki* [1991]
K_{iO2}	Inhibition constant for fermentation and acetogenesis	[g C m^{-3}]		(A9)	*Grant et al.* [2007]
n	Number of microbes per unit soil mass	[g^{-1}]	2.4×10^{-12}	(A5b)	*Grant and Pattey* [2003]
R	Gas constant	[J mol^{-1} K^{-1}]	8.3143	(A10b)	*Campbell* [1985]
R_m	Specific maintenance respiration at 25°C	[g C g N^{-1} h^{-1}]	0.0115	(A13)	*Barnes et al.* [1998]
RQ_{O2}	Respiratory quotient	[g C g O^{-1}]	0.375	(A4), (B4)	*Brock and Madigan* [1991]
R'_e	Specific respiration of heterotrophic aerobes $M_{i,n,a}$ *(n = e)* at 25°C, Nonlimiting hydrolytic products [$Q_{i,C}$], N and P microbial contents, O_2	[g C g MC^{-1} h^{-1}]	0.15	(A3), (A4)	*Grant et al.* [1993a, 1993b]
R'_f	Specific respiration of fermenters and agetogens $M_{i,f,a}$ *(n = f)* at 30°C, at high water potential, nonlimiting [$Q_{i,C}$], N and P microbial contents	[g C g MC^{-1} h^{-1}]	0.4	(A9)	*Wofford et al.* [1986]

Table 1. (continued)

Term	Definition	Unit	Value	Relevant Equation	Reference
R'_m	Specific respiration of acetotrophic methanogens $M_{i,m,a}$ ($n = m$) at 30°C, at high water potential, nonlimiting $[A_{i,C}]$, N and P micr. cont.	[g C g MC^{-1} h^{-1}]	0.2	(A11)	*Smith and Mah* [1980]
R'_c	Specific plant autotrophic respiration of $\varsigma_{ci,lz}$ at 25°C	[g C g C^{-1} h^{-1}]	0.015	(B3), (C2)	*Grant* [1989]
R'_{mp}	Specific plant maintenance respiration of $\varsigma_{ci,lz}$ at 25°C	[g C g N^{-1} h^{-1}]	0.0115	(B2), (C4)	*Barnes et al.* [1998]
r_m	Radius of a microbial sphere	[m]	10^{-6}	(A5b)	*Grant and Pattey* [2003]
S'_{O2}	Ostwald solubility coefficient for O_2	[g O_{2A} m^{-3} (g O_{2G} $m^{-3})^{-1}$]	0.029	(D5), (E3)	*Wilhelm et al.* [1977]
ν_g	Power function of gaseous diffusivity in soil	[-]	2.3	(D2a)–(D2c)	*Campbell* [1985]
ν_p	Power function of gaseous diffusivity in roots	[-]	1.33	(E2)	*Luxmoore et al.* [1970a]
θ_p	Plant root porosity	[m^3 m^{-3}]	0.1	(E2)	*Luxmoore et al.* [1970b]
λ	Hydrodynamic dispersion coefficient	[m]	4×10^{-3}	(D4a)–(D4d)	*Bresler* [1973]
ψ_t	Plant turgor below which organ extension stops	[MPa]	0.2	(B6)	*Klepper* [1990]
σ'_{O2AS}	Aqueous diffusivity of O_2 ($\gamma = O_2$)	[m^{-2} h^{-1}]	8.6×10^{-6}	(D4a)–(D4d)	*Campbell* [1985]
σ'_{O2GS}	Gaseous diffusivity of O_2 ($\gamma = O_2$)	[m^{-2} h^{-1}]	6.4×10^{-2}	(D2a)–(D2c)	*Campbell* [1985]

[13] Model equations for microbial hydrolysis and microbial and root respiration and growth are connected to simulated soil hydrology, directly through soil water content θ, and indirectly through aqueous and gaseous O_2 and their transfer and transport through water and gas phases in peat [*Grant*, 2001]. Also, these equations are connected to simulated conductive-convective heat flux in soil, coupled to soil hydrology [*Grant*, 2001] and further elaborated for peat as a porous media [*Dimitrov et al.*, 2010b]. Thus, the equations for microbial and root respiration and growth, as well as those for O_2 transport and transfer, are controlled by soil temperatures, determined by soil heat flux, in the course of the entire year including autumn/winter freezing, early spring thawing and growing season. Below we summarize only the key model algorithms that are unique for testing the hypotheses of this study.

2.1. Organic Matter Transformations, Microbial Hydrolysis, Respiration, and Growth

[14] Organic transformations in *ecosys* occur in each soil layer l in five organic matter-microbe complexes i, i.e., coarse woody litter, fine nonwoody litter, animal manure, particulate organic matter (POM), and humus. Each complex consists of five organic states, i.e., solid organic matter, dissolved organic matter, including acetate for methanogenesis, sorbed organic matter, microbial biomass and microbial residues, among which carbon (C), nitrogen (N), and phosphorus (P) are transformed. Organic matter in plant litter and manure are partitioned from proximate analysis into four kinetic components, i.e., carbohydrate, protein, cellulose, and lignin, each of which has different vulnerability to hydrolysis. Organic matter in POM, humus, microbial biomass and microbial residues in all complexes are also partitioned into components of different vulnerability to hydrolysis. Microbial biomass and residues are partitioned into labile and resistant structural components. Organic N and P uptake/release, inorganic N and P mineralization/immobilization, and N_2 fixation are driven by gains and losses of microbial C [*Grant et al.*, 2007].

[15] Active microbial biomass M_a of all heterotrophic microbial populations controls the rates of hydrolysis of each component of each organic state in each complex, which also depend through first-order Monod functions on substrate concentrations and are controlled by an Arrhenius function for temperature sensitivity equations (A1a)–(A1c)). The inhibitory effect of desiccation upon hydrolysis, through competitive inhibition of microbial exoenzymes [*Lizama and Suzuki*, 1991] considered to vary with the active microbial biomass [*Grant*, 2001], is caused by increase of aqueous microbial concentrations $[M_a]$ with decrease of soil water content at each soil layer θ_l (equation (A2)). As C hydrolysis products Q are the substrate for heterotrophic respiration R_h, the above algorithm describes the immediate effect of soil drying on R_h.

[16] Total R_h for all soil layers, plus CO_2 production from methanotrophs [*Grant and Roulet*, 2002] minus catabolic CO_2 production by autotrophic methanogens [*Grant*, 1998a, 1998b; *Grant and Roulet*, 2002] and anabolic CO_2 consumption by nitrifiers [*Grant and Pattey*, 2003, 1999], drives CO_2 emission from the soil surface through volatilization and diffusion. The CO_2 emission from all the microbial populations is controlled by soil temperature through an

Arrhenius function and by microbial N and P [*Grant et al.*, 2007]. Active biomass of aerobes $M_{e,a}$ controls the aerobic respiration $R_{h,e}$, which directly depends through Michaelis-Menten kinetics on concentration of C hydrolysis products [Q] and is controlled by microbial O_2 uptake (equation (A3)) with respect to microbial O_2 demand (equation (A4)). The O_2 uptake is constrained by ambient aqueous O_2 concentrations [O_{2AS}] and dispersivity-diffusivity (equations (A5a) and (A5b)), determined by gaseous O_2 concentrations and dispersivity-diffusivity [*Grant*, 2004, 2001]. Biomass growth yield, which drives biomass growth of aerobes, is determined from the energy yield of aerobic oxidation and the energy requirement for microbial biosynthesis (equation (A6)). The above algorithm determines the immediate increase of $R_{h,e}$ with receding WT through promoting gaseous O_2 diffusion in peat air-filled pores, by which aqueous O_2 in the water-filled pores is rapidly replenished.

[17] Contribution of autotrophic methanotrophs to CO_2 production is also restricted by O_2, but methanotrophs do not depend on hydrolysis, hence are not affected by desiccation [*Grant and Roulet*, 2002]. During soil wetting decrease of O_2 diffusion creates demand for electron acceptors unmet by O_2. R_h not coupled with O_2 reduction is coupled with sequential reduction of NO_3^-, NO_2^- and N_2O by facultative denitrifiers (equations (A7) and (A8)), with reduction of C by fermenters and H_2-producing acetogens in syntrophy with H_2-consuming methanogens (equation (A9) and equations (A10a) and (A10b)), and with reduction of C by acetotrophic methanogens (equations (A11) and (A12)). The inhibiting effect of O_2 confines fermentation to highly waterlogged conditions and is quantitatively expressed through the soil aqueous O_2 concentration [O_{2AS}] (equation (A9)). Thus, receding WT indirectly promotes $R_{h,e}$.

[18] All microbial populations undergo maintenance respiration R_m, depending on microbial N and temperature (equation (A13)). R_h in excess of R_m is used as growth respiration R_g (equation (A14)), which drives microbial uptake U of C hydrolysis products Q through microbial biomass growth yield Y (equation (A15)). R_m in excess of R_h causes microbial dieback, which is expressed as decomposing microbial C D_M (equation (A16)). Thus, the change of microbial C δM, i.e., microbial growth, for each model time step δt, is calculated from gains by U minus losses by R_m, R_g and D_M (equation (A17)). Hence, active microbial biomass M_a, conducting hydrolysis and heterotrophic respiration, and associated with each organic matter-microbe complex, is calculated from all the heterotrophic populations as a sum of the labile and resistant microbial C, partitioned between the labile and resistant structural components (equation (A18)). Thus, with low WT and near-surface drying respiring microbial biomass in the upper peat will equilibrate in time at low values through limited hydrolysis, while respiring microbial biomass in deeper, well aerated peat above the water table will equilibrate in time at high values with rapid replenishment of aqueous O_2 in water-fillled pore space.

2.2. Root Respiration and Growth, Aboveground Plant Respiration

[19] Total root respiration $R_{a,P}$ is generated from respiration R_c of root nonstructural carbon (equation (B1)) that is product of photosynthesis and nonstructural C transfer driven by concentration gradients that arise from C fixation in shoots and C oxidation in shoots and roots [*Grant et al.*, 2007]. Whenever R_c alone cannot meet the demand for root maintenance respiration, which depend on root N and temperature, the shortfall is generated from respiration of root remobilized carbon R_s (equations (B1) and (B2)), which drives root litterfall. The R_c is controlled by temperature, nutrients and root O_2 uptake (equation (B3)) with respect to root O_2 demand (equation (B4)). The root O_2 uptake is consrained by aqueous O_2 concentrations at root and myccorhizal surfaces [O_{2AR}] (equation (B5a)). The [O_{2AR}] is concurrently controlled by ambient aqueous O_2 concentrations and dispersivity-diffusivity in soil (equation (B5b)), and in roots (equation (B5c)), which are controlled by gaseous O_2 concentration and dispersivity-diffusivity in soil and root air-filled porosities [*Grant*, 2004, 1998a, 1993]. Thus, root respiration may be immediately constrained by low soil and root air-filled porosities in wet soils.

[20] Excess (if any) of R_c above the maintenance respiration is expended as root growth respiration that is controlled by the excess of the root turgor potential ψ_t above a threshold value below which organ extension stops (equation (B6)). The root growth respiration determines root nutrient uptake, hence growth of root biomass, as a difference between gains through nutrient uptake and losses through growth and maintenance respiration, and litterfall (equation (B7)). Thus, respiring root biomass is constrained by low soil water content θ through ψ_t. All model algorithms for C transformations in roots are replicated for mycorrhizae, which exchange nonstructural C, N and P with roots [*Grant*, 2001]. Total autotrophic aboveground respiration $R_{a,A}$ is calculated in the same way as $R_{a,P}$, except that $R_{a,A}$ is not limited by O_2 (equations (C1)–(C4)). However, the nonstructural C pool from which $R_{a,A}$ is generated varies with plant productivity, which varies with θ through soil-plant water relations [*Grant*, 2001].

3. Site Description

[21] Mer Bleue bog is a large (~28 ha), ombrotrophic bog, located about 15 km east of Ottawa in Ontario, Canada. The ground cover is mainly *Sphagnum* mosses and overstory vegetation is dominated by a low shrub canopy (20–30 cm height), with sparse sedges and herbaceous plants and some discontinuous patches of coniferous trees [*Lafleur et al.*, 2005a; *Frolking et al.*, 2002; *Moore et al.*, 2003]. Peat depth increases from 2 to 6 m from the periphery toward the center and is about 4–5 m deep around the eddy-covariance (EC) tower [*Lafleur et al.*, 2005b]. The bog surface has expressed hummock-hollow microtopography, dominated by hummocks with an average diameter of 1 m that comprise about 70% of the surface, and an average relief between hummocks and hollows of 25 cm [*Lafleur et al.*, 2005b]. Mer Bleue is a dry peatland with WT varying between ~20 and ~70 cm below the hummock surface [*Lafleur et al.*, 2005a, 2005b]. Based on peat texture and Von Post degree of humification, fibric peat occupies the top 0–35 cm, then hemic peat at 35–45 cm, and sapric peat at >45 cm in hummocks, and at 0–10 cm, 10–20 cm, and >20 cm, respectively, in hollows [*Lafleur et al.*, 2005b; S. Admiral, personal communication,

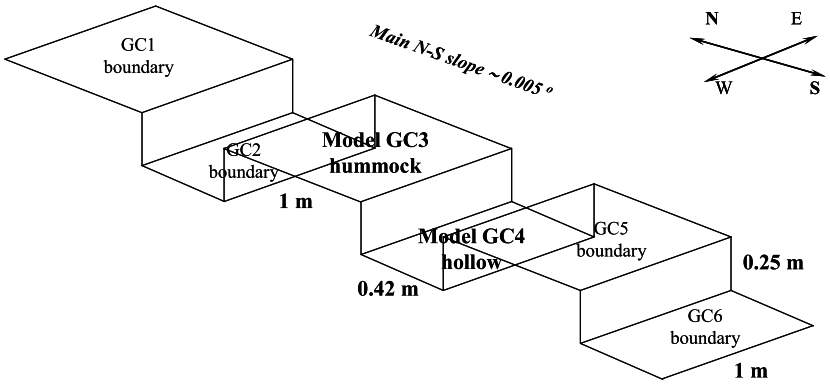

Figure 2. Model 3-D transect with specific microtopography at Mer Bleue bog, as represented in *ecosys*.

2005]. Macroporosity of fibric peat is estimated to be 0.8 m^3 m^{-3} [*Dimitrov*, 2009].

4. Methods

4.1. Model Experiment

[22] To test the hypotheses for the effects of varying WT and θ on ecosystem respiration, a model transect of 6 grid cells, consisting of 3 hummocks and 3 hollows, was designed to represent the microtopography of Mer Bleue bog (Figure 2). Water and gaseous fluxes in the model were shut off in east-to-west direction with a slope of 0.0008°, negligible for the scale of this research, and were allowed only in north-to-south direction following the main slope of the terrain, and in vertical direction. The hourly model output used in comparisons with measured and literature data was generated from the third and fourth cells, representing bog hummocks and hollows, respectively; the first and second, and the fifth and sixth cells were considered as boundary cells. Key soil properties for Mer Bleue bog are summarized in Figure 1. *Ecosys* was run for 106 years in which the model was initialized with the biological properties of shrub and moss, and spun up by repeating 15 times the 7 year available weather period of 1998–2004. Equilibrium during the model spin up was attained after 60–70 years, when changes in simulated C sequestration in the soil humic pool became stable over time [*Ju et al.*, 2006]. The same model run has already been applied to simulate subsurface peat hydrology and peat thermal regime at Mer Bleue bog in previous studies [*Dimitrov et al.*, 2010a, 2010b]. For consistency, the WT level in this study is always referenced to the hummock surface for both hummocks and hollows.

4.2. Corroborating Modeled Soil Respiration Versus Indpendent Laboratory and in Situ Experimental Studies

[23] Previous research on hummocks at Mer Bleue bog was used to evaluate the modeled response of near-surface soil respiration to hydrological constraints. Peat cores were collected from depths 0–5 cm and 10–15 cm in hummocks, allowed to dry over 10 days, and then rewetted to ~40–50% on volumetric basis, i.e., well above their field capacity, and then subjected to three drying cycles of 10 days each at constant temperature of 20°C in the laboratory [*Lafleur et al.*, 2005a; T. Moore, personal communication, 2008].

[24] It was assumed that after 20 days, i.e., the first two drying cycles, the respiration during the third drying cycle (between days 20 and 30) was mainly microbial with no residual root activity. Under this assumption, microbial respiration of peat at 0–5 cm and 10–15 cm depths during this third drying cycle at 20°C was numerically expressed as peat CO_2 production (g C m^{-3} h^{-1}) regressed on peat θ (% on volumetric basis) (regression equations from T. Moore, personal communication, 2008). These regressions were then used with in situ time domain reflectometry (TDR) measurements of peat θ (%) at Mer Bleue to estimate volumetric microbial respiration rates of peat at 20°C for periods with contrasting WT depths. For comparison with modeled values, the respiration rates were then adjusted for in situ peat temperature by applying another regression equation between in situ soil respiration (g C m^{-2} h^{-1}) and peat temperature (°C) at 5 cm and 10 cm depths in hummocks at Mer Bleue bog [*Lafleur et al.*, 2005a]. The adjusted respiration rates were then compared with modeled respiration rates at the corresponding depths in the simulated peat profile.

[25] Respiration rates modeled below the fibric peat zone in hummocks (depth >35 cm) were compared with experimentally derived anaerobic respiration rates from hummock peat at 40 cm depth in Mer Bleue bog [*Scanlon and Moore*, 2000], adjusted for soil temperature. Similarly, rates modeled below 50 cm depth in hollows were compared with the maximum reported anaerobic respiration rates below 50 cm in Mer Bleue hollows [*Blodau et al.*, 2007].

4.3. Testing Modeled ER Versus Field Studies

[26] After testing of simulated microbial respiration against the experimental findings described in section 4.2 and after investigating simulated root and aboveground respiration, the total bog ER was compared to EC-measured and gap-filled ER at hourly, hourly binned (over 30 day periods) and annual timescales. To test hourly simulated versus EC-measured ER, 10 day periods (end of June) were selected with higher and lower WT in 2002 and 2001, respectively. These specific periods were selected because they contained relatively little missing EC-measured CO_2 efflux data. Hourly binned EC and simulated ER were compared during 30 day periods in August–September 2001 and 2004, with low and intermediate average WT (measured and simulated), respectively. Hourly binned soil respiration was investigated and tested under contrasting WT during the above periods, and also

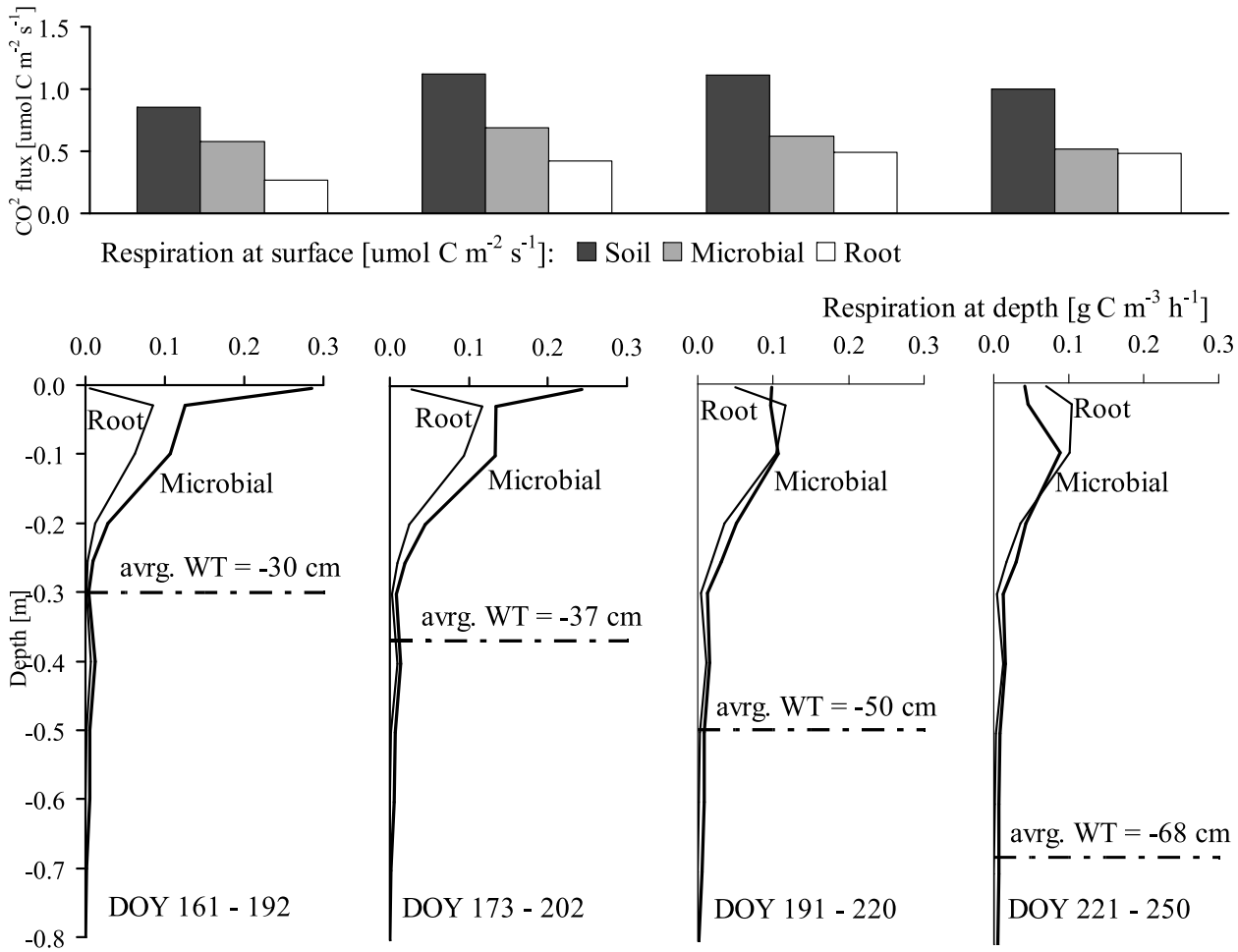

Figure 3. Average simulated microbial and root CO_2 production at depth in hummocks, associated with the WT drawdown in the course of the vegetation season, Mer Bleue bog, DOY 161–250, year 2002. Vertical axis refers to depth from hummock surface.

during 30 day periods during June–July 2001 and 2000, with intermediate and high average WT, respectively. Simulated versus Finally, EC-derived annual ER was compared for a wet year 2004 and a dry year 2001 with high and low average WT depths, respectively.

[27] The simulated hourly nighttime ER was regressed on the EC-measured hourly CO_2 efflux with friction velocities $u_* > 0.1$ m s^{-1} [*Lafleur et al.*, 2003] for the period 2000–2004. Discrepancy between model output and measurements were evaluated by the root mean square deviation (RMSD) and mean absolute error (MAE), and relative discrepancy by Willmott's index of agreement [*Willmott*, 1982, 1981; *Davies*, 1981; *Powell*, 1980; *Willmott and Wicks*, 1980]. To evaluate goodness of fit and predictive power of the model, coefficients of determination, slopes and intercepts were obtained from a linear regression between modeled hourly nighttime ER and EC-measured hourly CO_2 efflux records.

5. Results

5.1. Effects of Water Table on Soil Respiration in Hummocks

[28] The most rapid WT drawdown at Mer Bleue within the 1998–2004 period occurred during the dry summer of 2002 with only 380 mm rainfall (May–September), one of the driest in the entire 7 year period [*Lafleur et al.*, 2005b]. To capture temporal patterns of soil respiration with depth, simulated average rates of microbial and root respiration were calculated for each soil layer over four 30 day periods during the water table decline: DOY 161–190, DOY 173–202, DOY 191–220 and DOY 221–250, respectively, with high, intermediate, moderately low and low average measured WT depths (Figure 3). Simulated microbial and soil (microbial + root) respiration were low at high WT depth (DOY 161–190), increased as water table dropped, approaching maximum values at WT depth of ~37 cm (DOY 173–202), and decreased again with deeper water table (DOY 191–220, DOY 221–250) (Figure 3). The most rapid microbial respiration in the model occurred at the intermediate WT depths (DOY 173–202), when moisture maintained rapid hydrolytic rates in the most productive near-surface peat, and increased oxygenation caused rapid microbial aerobic respiration at depth, above the water table. Simulated root respiration generally increased with increased soil aeration; the slight decrease late in the growing season (DOY 221–250) was due to decreased root biomass in the model. To further elucidate the effects of WT depth on soil respiration representative periods of intermediate

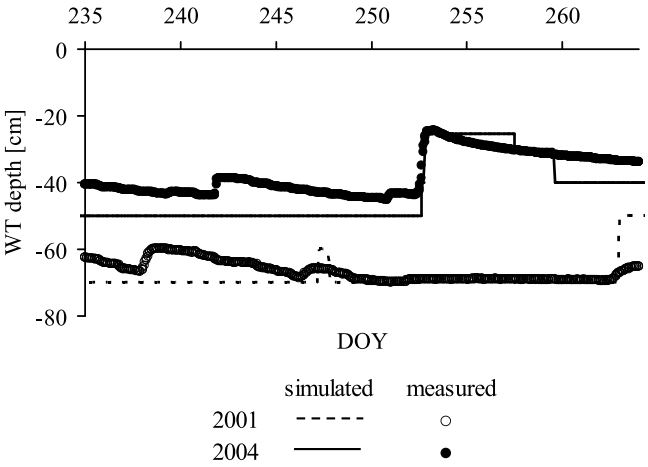

Figure 4. Hourly simulated and measured (potentiometric) WT depths from the hummock surface at Mer Bleue bog, DOY 235–264, dry year 2001 versus DOY 235–264, wet year 2004.

versus both low and high WT depths are compared below. These periods with similar environmental conditions but with contrasting hydrology were chosen from different years to minimize seasonal effects other than WT on respiration rates.

5.1.1. Intermediate Versus Low Water Table

[29] DOY 235–264 in 2001 and 2004, with similar incoming short-wave radiation and air and soil temperatures, provided an opportunity to contrast respiration in hummocks with low and intermediate WT (Figure 4) and associated θ, respectively (Figures 5a and 5b). The simulated soil respiration rate in hummocks was 0.85 μmol CO_2 m^{-2} s^{-1} for DOY 235–264 for both the dry year 2001 and the wet year 2004, with average measured WT of ~ −67 cm and ~ −38 cm, respectively. Periods DOY 235–264 in 2001 and 2004 are referred to by year only in this section.

[30] The upward water flux modeled in highly macroporous and ~ 35 cm thick fibric peat in hummocks (Figure 1) was insufficient to keep the soil wet in 2001. With drying of the near-surface (0 to 5–10 cm) peat in 2001 (Figure 5a) θ was <25% of its micropore fraction (Figures 1 and 5a), which inhibited simulated hydrolysis by increasing aqueous concentrations of active microbial biomass [M_a] (equations (A1a) and (A1b) and equation (A2)). This resulted in lowered concentrations of hydrolytic products and therefore lowered aerobic heterotrophic respiration R_h (equation (A3)) (Figure 6a). Lower R_h, reduced microbial uptake U of hydrolitic products (equation (A15)), thus biomass growth rate (equation (A17)), and hence active microbial biomass M_a (equation (A18)), further lowering near-surface R_h (Figure 6a) and associated O_2 consumption (Figure 6b). However, increased O_2 transport with WT drawdown (Figure 4) increased R_h below the zone of near-surface desiccation (Figure 5a). With no water limitation, rapid replenishment of aqueous O_2 in well aerated fibric peat between 10 and 35 cm depth, and high energy and biomass yields from aerobic redox reactions (equation (A6)), caused rapid increase of R_h by increasing the active microbial O_2 uptake (equations (A5a) and (A5b)). More rapid R_h increased aerobic U of hydrolitic products (equation (A15)) and thus microbial biomass growth rate (equation (A17)) and M_a (equation (A18)), further increasing R_h (Figure 6a) and associated O_2 consumption (Figure 6b) between 10 and 35 cm depth. Water retention in hemic and sapric peat (Figure 5a) and limited rise of aqueous O_2 with WT drawdown constrained increase in R_h and O_2 consumption below 35 cm depth in 2001 (Figures 6a and 6b).

[31] During the wetter 2004, simulated near-surface θ remained >70% of the fibric peat micropores (Figures 1 and 5a), hence there were no desiccation effects on R_h, which was consistently ~7 times higher than in 2001. The R_h was slightly lower at ~30 cm in 2004 than in 2001 (Figure 6a), due to slower O_2 transport during temporary saturation after rainfall on DOY 253, with WT rise above 30 cm. The R_h from the well aerated and moist fibric peat between 10 and 30 cm depth (Figure 5a) was similar in 2001 and 2004 (Figure 6a). However, deeper gaseous O_2 diffusion with deeper WT drawdown in 2001 (Figure 4) increased R_h and O_2 consumption in hemic and sapric peat, compared to that in 2004 (Figures 6a and 6b).

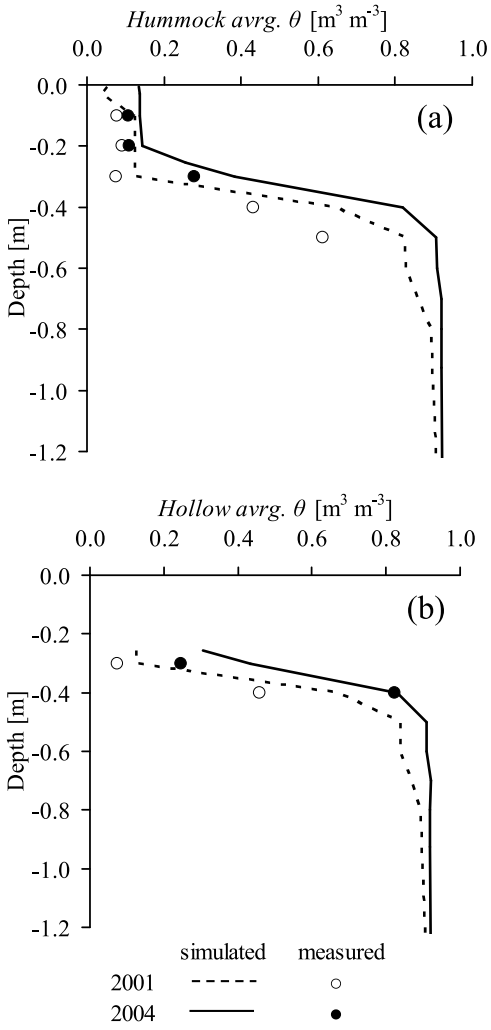

Figure 5. Average simulated and measured (TDR) soil water contents (θ) at depth in (a) hummocks and (b) hollows at Mer Bleue bog, DOY 235–264, dry year 2001 versus DOY 235–264, wet year 2004. Vertical axis refers to depth from hummock surface.

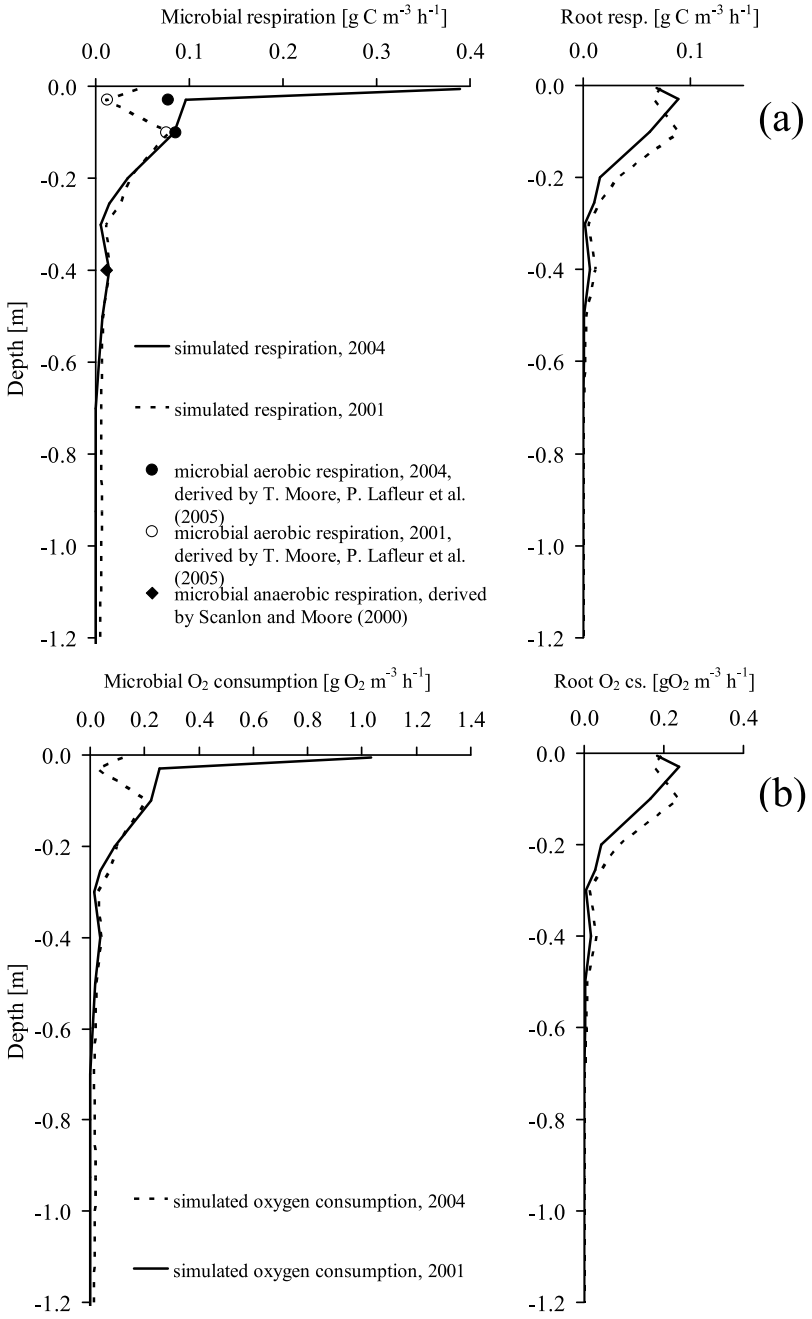

Figure 6. (a) Average (left) microbial and (right) root respiration at depth and (b) O_2 consumption at depth, hummock, Mer Bleue bog, DOY 235–264, dry year 2001 versus DOY 235–264, wet year 2004. Vertical axis refers to depth from hummock surface.

[32] In deep and saturated sapric peat severe O_2 depletion in the model stimulated anaerobic respiration mainly through acetogenic fermentation and acetotrophic methanogenesis (equations (A9) and (A11)). Low energy yields and hence biomass growth from anaerobic respiration (equations (A10a) and (A10b) and equation (A12)) caused slow uptake of hydrolytic products by anaerobes (equation (A15)), further slowing microbial biomass growth (equation (A17)), causing low active biomass M_a of anaerobes (equation (A18)). The low M_a of anaerobes and low substrate quality caused low simulated hydrolytic and respiration rates in deep peat for both 2001 and 2004 (Figure 6a).

[33] Total simulated root respiration $R_{a,P}$ in the wet 2004 was 86% of that in the dry 2001 (Figure 6a). Moss rhizoids were simulated to a depth of 5 cm only [*Richardson*, 1981]. Near-surface desiccation in 2001 (Figure 5a) caused decrease of near-surface soil water potentials, resulting in low rhizoid and near-surface vascular root turgor potentials ψ_t. Low ψ_t reduced rhizoid and near-surface root growth (equations (B6) and (B7)), hence respiration in the model in 2001 (equation (B1)), compared to those in 2004 (Figure 6a). However, extending the depth of the O_2 gaseous phase with WT drawdown in 2001 increased soil O_2 concentrations, hence root O_2 uptake (equations (B5a)–(B5c)) and respiration

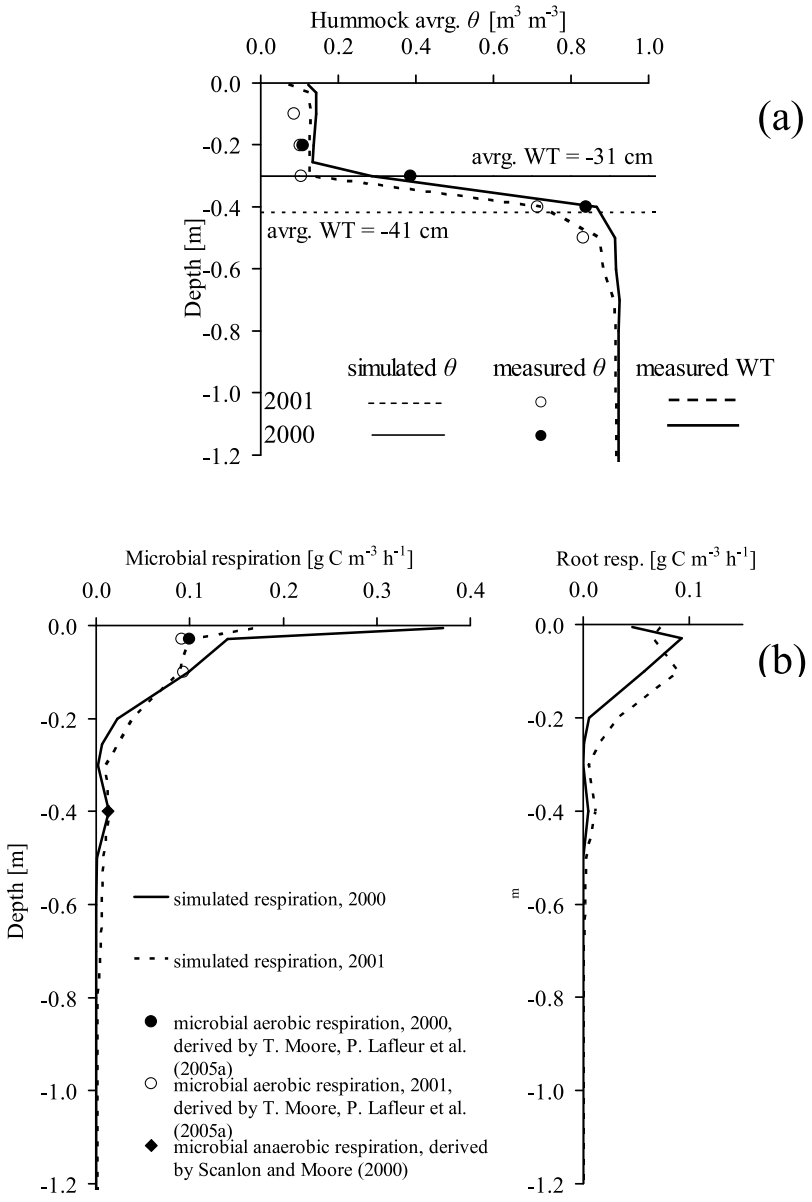

Figure 7. (a) Average measured and simulated water contents (θ) at depth, associated with measured WT, and (b) average (left) microbial and (right) root respiration at depth, hummock, Mer Bleue bog, DOY 173–202, dry year 2001 versus DOY 173–202, wet year 2000. Vertical axis refers to depth from hummock surface.

(equations (B3) and (B1)), which raised root biomass (equations (B6) and (B7)) compared to that in 2004. Simulated annual root respiration was 35% of the simulated annual soil respiration in 2004 and 46% of that in 2001, consistent with reported root respiration at a peatland in central Finland [*Silvola et al.*, 1996b].

5.1.2. Intermediate Versus High Water Table

[34] Periods DOY 173–202 in 2000 and in 2001 (average measured WT of ~ −31 cm and ~ −41 cm, respectively), subsequently referred to by year only in this section, provided an opportunity to contrast respiration in hummocks with high and intermediate WT (Figure 7a), given that other environmental factors were similar. Simulated soil respiration differed little and was 0.81 μmol CO_2 m^{-2} s^{-1} in 2000 and 0.95 μmol CO_2 m^{-2} s^{-1} in 2001. The lower water table in 2001 caused some decline of the near-surface θ (Figure 7a) that resulted in inhibition of simulated microbial activity and respiration, compared to that in 2000 (Figure 7b). At the same time, an increase in the air-filled porosity at depth in 2001 caused higher simulated soil respiration at depth, compared to that in 2000 (Figure 7b).

5.2. Effects of Water Table on Soil Respiration in Hollows

[35] In contrast to hummocks, shallower WT and shallower fibric peat in hollows (Figure 1) resulted in sustained capillary rise from the hemic and sapric peat of high water retention [*Nazaroff*, 1992] up to the relatively close hollow surface that prevented near-surface drying in hollows (Figure 5b). Thus, the average soil respiration in hollows increased with

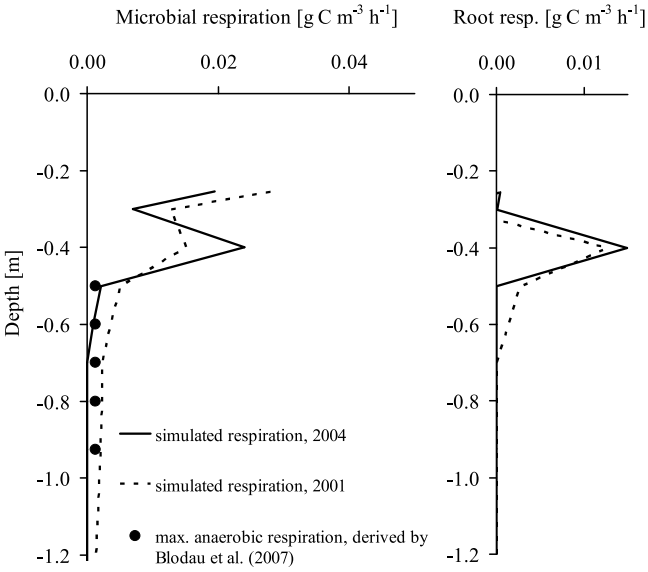

Figure 8. Average (left) microbial and (right) root respiration at depth, hollow, Mer Bleue bog, DOY 235–264, dry year 2001 versus DOY 235–264, wet year 2004. Vertical axis refers to depth from hummock surface; the hollow surface is located 25 cm below the hummock surface.

WT drawdown during DOY 173–202 from 0.03 μmol CO_2 m^{-2} s^{-1} in 2000 (average WT ~ −31 cm) to 0.11 μmol CO_2 m^{-2} s^{-1} in 2001 (average WT ~ −41 cm) and during DOY 235–264 from 0.12 μmol CO_2 m^{-2} s^{-1} in 2004 (average WT ~ −38 cm) to 0.14 μmol CO_2 m^{-2} s^{-1} in 2001 (average WT ~ −67 cm); simulated microbial and root respiration at depth during the latter period is given on Figure 8. The increase was more pronounced during DOY 173–202 when the water table receded below the macroporous fibric peat (Figure 1) and less pronounced during DOY 235–264 when the water table receded within the sapric peat of high water retention [*Lafleur et al.*, 2005a]. Waterlogged hollow peat suppressed aerobic and favored anaerobic microbial respiration and fermentation (equation (A9)), and reduced root biomass and respiration. Thus, simulated soil respiration in hollows was ~7 times less than that in hummocks and occurred on less than 1/3 of the bog total surface area (Figure 2). However, soil respiration in hollows may contribute more to the total soil respiration of other bogs with greater hollow: hummock surface ratios and deeper WT drawdowns, compared to those at Mer Bleue.

5.3. Effects of Water Table on Aboveground Plant Respiration

[36] The average simulated aboveground plant respiration $R_{a,A}$ declined with soil drying during DOY 173–202 from 2.04 μmol CO_2 m^{-2} s^{-1} in 2000 (average WT ~ −31 cm) to 1.88 μmol CO_2 m^{-2} s^{-1} in 2001 (average WT ~ −41 cm), and during DOY 235–264 from 1.60 μmol CO_2 m^{-2} s^{-1} in 2004 (average WT ~ −38 cm) to 1.37 μmol CO_2 m^{-2} s^{-1} in 2001 (average WT ~ −67 cm). This decline occurred for hummocks and was mainly due to decrease of the moss aboveground respiration with decrease of moss productivity, caused by reduction of the soil and moss water potentials in the model [*Dimitrov*, 2009]. Reduced productivity constrained aboveground respiration of moss through reducing nonstructural and remobilized carbon (equations (C1)–(C3)). Vascular productivity, hence aboveground respiration were not affected by near-surface desiccation in hummocks as shrubs compensated for reduced near-surface root water uptake with deeper root water uptake [*Dimitrov*, 2009]. Plant productivity and $R_{a,A}$ did not change with WT variation in the highly waterlogged peat in the hollows. Simulated aboveground respiration was 47% and 49% of the ecosystem respiration for 2001 and 2004, similar to the 50% simulated by PCARS model [*Frolking et al.*, 2002].

5.4. Testing of Modeled ER Under Varying WT Versus Field Studies

5.4.1. Hourly Bog ER

[37] Model findings in previous sections could not be tested at an hourly level during the above periods due to scarcity of hourly EC-measured CO_2 efflux records with friction velocities $u_* > 0.1$ m s^{-1}, the threshold used to accept EC CO_2 fluxes at Mer Bleue bog [*Lafleur et al.*, 2003]. To investigate the effects of WT variation on bog ER at an hourly level, the periods DOY 176–187 in 2002 and 2001 were selected because of the high number of accepted hourly CO_2 efflux records. Both simulated and measured WT in 2002 were higher than those in 2001 during DOY 176–183, as simulated WT converged and measured WT converged after DOY 185 (Figure 9a). Also, simulated and measured nighttime soil temperatures T_S were similar before DOY 182, then diverged and converged again on DOY 186 (Figure 9b), thus giving an opportunity to observe some combined WT and T_S effects on bog ER. Nights with the most hourly CO_2 efflux records were chosen to investigate ecosystem respiration with (1) contrasting WT and similar T_S (DOY 177–178 and DOY 181–182), (2) contrasting WT and contrasting T_S (DOY 182–183), and (3) similar WT and similar T_S (DOY 186–187) (Figure 9c).

[38] For both 2002 and 2001 ecosystem respiration was similar during DOY 177–178 and DOY 181–182 despite contrasting WT and similar T_S (Figures 9a–9c). The ecosystem respiration was also similar during DOY 186–187 with similar WT and T_S in the two years (Figures 9a–9c), suggesting that the WT variation did not affect ER. However, both simulated and measured ER rose pronouncedly with T_S (Figure 9b) during DOY 182–183 and the following three nights (Figure 9c), suggesting that the T_S is the main control over ecosystem respiration at Mer Bleue bog rather than the water table, as suggested by *Lafleur et al.* [2005a] too. Simulated hourly ER corresponded well to EC-measured one at Mer Bleue bog ranging from ~1 μmol CO_2 m^{-2} s^{-1} in early spring and late autumn to ~2 to 4 μmol CO_2 m^{-2} s^{-1} in midsummer [*Lafleur et al.*, 2005a].

[39] The hypothesis that WT variation has little effect on bog ER was independently confirmed by measurements alone (Figures 9a and 9c). The average absolute differences between the hourly CO_2 efflux records on DOYs 176–177, 181–182 and 186–187 in 2002 and those in 2001, with different WT but similar T_S, were 0.85, 1.06 and 1 μmol CO_2 m^{-2} s^{-1}, which were less than or equal to 1.06 μmol CO_2 m^{-2} s^{-1} that was estimated to be the maximum random error of EC-measured hourly CO_2 efflux at Mer Bleue bog, derived from *Richardson et al.* [2006]. However, the average

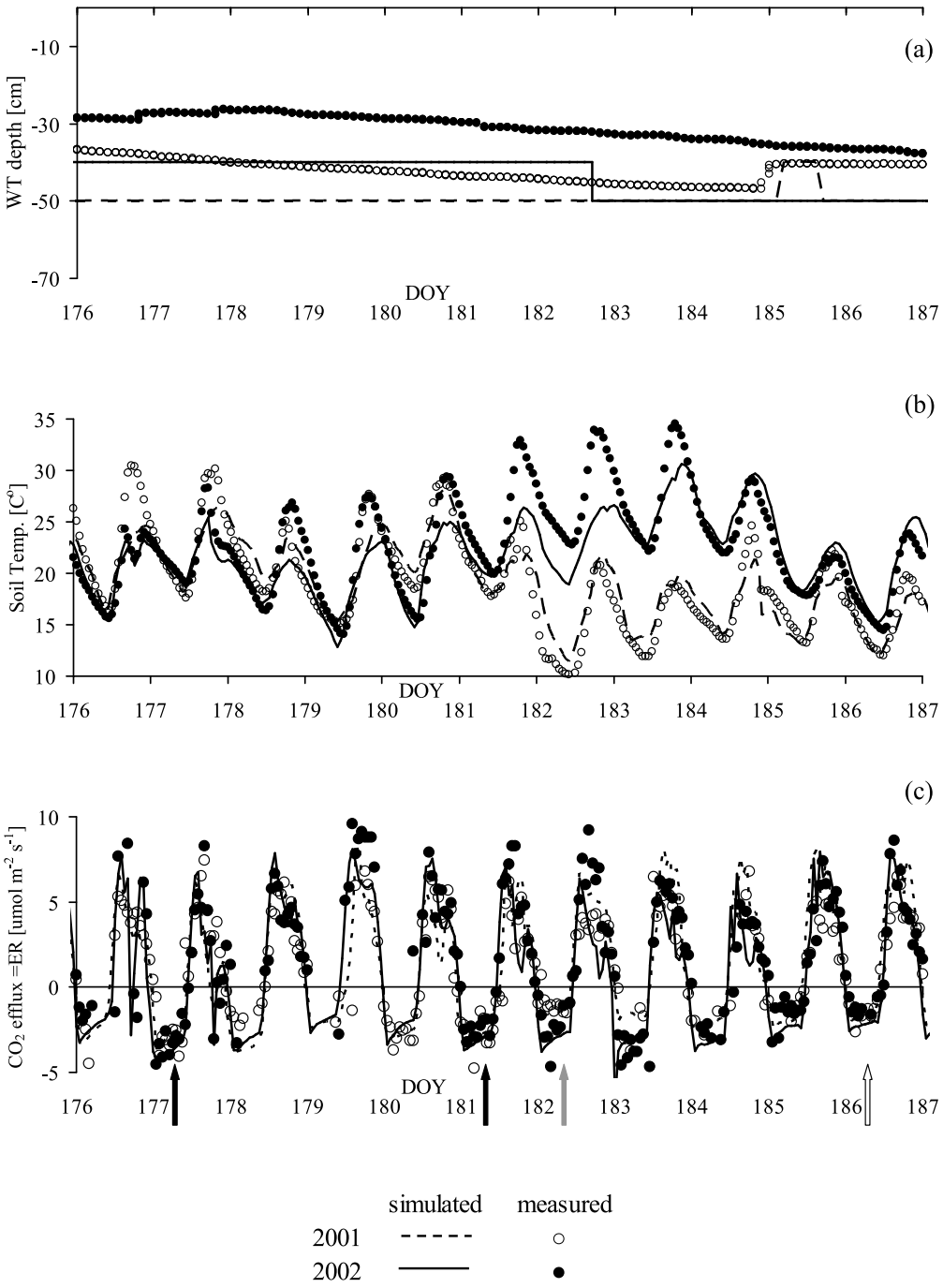

Figure 9. Hourly simulated and measured (a) WT, (b) soil temperatures at 5 cm below hummock surface, and (c) CO_2 flux, Mer Bleue bog, dry year 2001 versus wet year 2002. Nighttime CO_2 efflux values (negative) represent ecosystem respiration. Black arrows indicate the CO_2 flux under contrasting hydrological conditions on DOY 178, DOY 182. White arrow indicates the CO_2 flux under similar hydrological conditions on DOY 187. Gray arrow indicates effects of soil temperature on the CO_2 flux on DOY 183. Vertical axis refers to depth from hummock surface.

absolute difference for DOY 182–183 between 2002 and 2001, under similar WT but different T_S, was 1.63 μmol CO_2 m^{-2} s^{-1}. As this value is significantly greater than the maximum random error noted above, the analysis suggests that the EC technique did not distinguish bog ER with varying WT, but did distinguish bog ER with varying T_S.

5.4.2. Hourly Binned Bog ER

[40] Simulated hourly binned bog ER over monthly periods of contrasting WT changed little with WT drawdown due to the respiration offset. Hourly binned ER was 2.01 μmol CO_2 m^{-2} s^{-1} during DOY 235–264 in 2001 (average WT ~ −67 cm), similar to 2.23 μmol CO_2 m^{-2} s^{-1} during the same

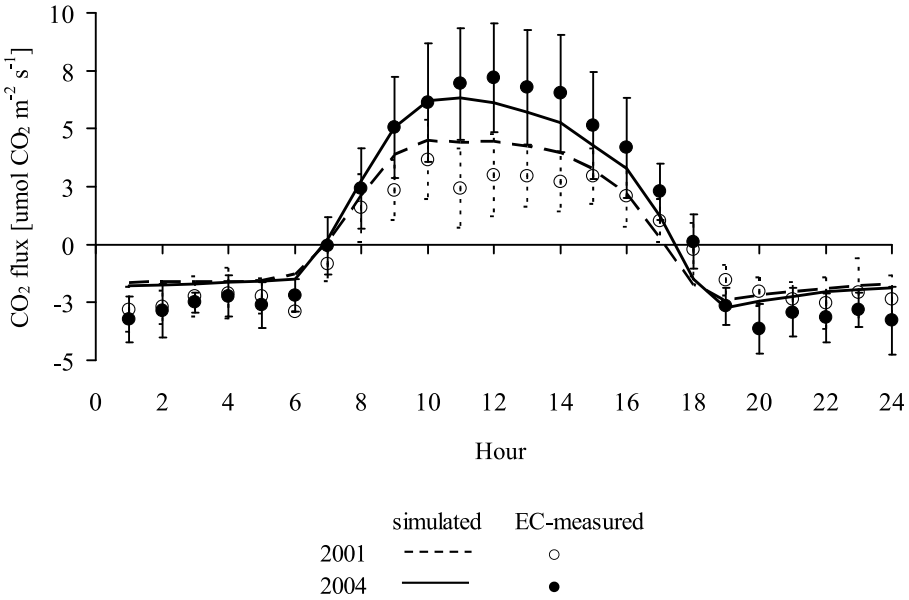

Figure 10. Hourly binned simulated and EC-measured CO_2 flux, Mer Bleue bog, DOY 235–264, dry year 2001 versus DOY 235–264, wet year 2004. Nighttime values (negative) represent ecosystem respiration. Bars indicate ± SD for EC-measured CO_2 flux.

period in 2004 (average WT ~ −38 cm), and 2.58 μmol CO_2 m^{-2} s^{-1} during DOY 173–202 in 2001 (average WT ~ −41 cm), similar to 2.62 μmol CO_2 m^{-2} s^{-1} during the same period in 2000 (average WT ~ −31 cm). Simulated hourly binned nighttime ER fell within one standard deviation of EC-measured CO_2 effluxes, indicating good agreement between simulated and measured ER (Figure 10). Furthermore, the EC-measured hourly binned CO_2 effluxes for 2001 and 2004 fell within each other's standard deviation (Figure 10), indicating similar ER measured by EC with contrasting WT.

5.4.3. Annual Bog ER

[41] Simulated ER of 658 g C m^{-2} yr^{-1} for the dry 2001 (average annual WT ~ −43 cm) and 623 g C m^{-2} yr^{-1} for the wet 2004 (average annual WT ~ −38 cm) fitted within the confidence intervals of the annual cumulative random errors (calculated according to *Griffis et al.* [2004]) of the EC-derived ER, i.e., 535 ± 134 g C m^{-2} yr^{-1} for 2001 and 578 ± 145 g C m^{-2} yr^{-1} for 2004. Thus, simulated ER and EC-derived ER were not significantly different during years with contrasting WT depths.

5.5. Agreement Between Modeled and Measured Soil Respiration and ER

[42] Sensitivity of microbial respiration to θ at near-surface peat in the model was consistent with sensitivity of the independently derived microbial respiration to TDR-measured θ (Figures 6a and 7b). The slope (0.74) of the regression of simulated ER on measured ER for 2000–2004 (Table 2) indicated that the model tended to underestimate the measured hourly CO_2 effluxes. A possible explanation was as follows. The low CO_2 flux values, with friction velocities below the threshold, were discarded during nights of low wind speed, such as DOY 176 and DOY 181 in 2001, and DOY 182 in 2004 (Figure 9c). However, sudden wind flushes might have possibly forced eddies with friction velocities above the threshold to carry the accumulated above-surface CO_2, which was detected as a large CO_2 emission in the field [*Falge et al.*, 2001] and was not captured by the model. Thus, the model underestimated measured only CO_2 effluxes, but at the same time overestimated measured plus gap-filled CO_2 effluxes together, which resulted in overestimated ER at an annual timescale. Yet, the intercept (Table 2) indicated that the model might sometimes be biased toward greater hourly CO_2 effluxes, especially when the measured ones tended to zero near sunrise when photosynthesis began to offset respiration.

[43] Willmott's index of agreement d indicated small relative discrepancy between modeled and measured ER (Table 2). Both root mean square difference (RMSD) and mean absolute error (MAE) between modeled and EC-measured nighttime hourly ER (Table 2) were less than 0.74 μmol CO_2 m^{-2} s^{-1}, estimated to be the random error of EC-measured hourly CO_2 effluxes at Mer Bleue bog for 2000–2004, derived from *Richardson et al.* [2006]. This gave some con-

Table 2. Statistics for a Regression of Simulated Nighttime Hourly Ecosystem Respiration on EC-Measured Nighttime Hourly CO_2 Exchange (Respiration) at Mer Bleue Bog for the Period 2000–2004

Statistics (n = 5424)	Units	Values (Significance)
Slope, b	–	0.74 ($p < 0.0001$)
Intercept, a	μmol CO_2 m^{-2} s^{-1}	−0.51 ($p < 0.0001$)
R^2	–	0.56 ($p < 0.0001$)
Willmott's d	–	0.85
RMSD	μmol CO_2 m^{-2} s^{-1}	0.66
MAE	μmol CO_2 m^{-2} s^{-1}	0.49

fidence that differences between simulated and EC-measured ER were smaller than uncertainty in EC-measured ER.

6. Discussion

[44] Recent studies have attempted to explain the lack of a strong response of ER to changes in WT depth at Mer Bleue bog largely in terms of these changes occurring in the zone of hemic and sapric peat with poor substrate quality, high water retention and limited oxygenation, which combine to limit increases/decreases in soil respiration with WT fall/rise [*Lafleur et al.*, 2005a]. Studies in other peatlands suggested that soil respiration was greatest and most sensitive to θ in the uppermost hummock peat [*Waddington et al.*, 2001; *Updegraff et al.*, 1995], and that soil respiration remained relatively unchanged in hummocks but increased in hollows with WT drawdown [*Strack and Waddington*, 2007]. Our research is consistent with these studies and builds upon their findings by simulating changes in θ of macroporous and productive fibric peat with WT drawdowns. Such changes cause increased soil respiration at depth in hummocks and hollows to be offset by decreased near-surface soil respiration and aboveground moss respiration at hummocks. Although conservative to WT variation, the ER was found to depend strongly on soil temperature, as previously suggested for the Mer Bleue bog [*Lafleur et al.*, 2005a, 2005b], for a fen and a bog in Minnesotta [*Updegraff et al.*, 2001], for a bog in Quebec [*Waddington et al.*, 2001], and for a bog in Ontario, a fen and a swamp in Quebec [*Moore and Dalva*, 1993].

6.1. Specific Peat Properties Behind the Respiration Offset in Peat Profile

[45] Simulated θ declined to ~0.03–0.05 m^3 m^{-3} in the uppermost 0 to 5–10 cm during DOY 235–264 in 2001 (Figure 5a). Near-surface desiccation disappeared at ~10 cm depth, below which θ was maintained at ~0.12 m^3 m^{-3} (Figure 5a) down to the bottom of the fibric peat, i.e., ~60–80% of its volumetric matrix fraction. The increase in modeled and measured θ to saturation (Figure 5a) in the hemic and sapric peat was associated with absence of macroporosity (Figure 1) and greater water retention [*Lafleur et al.*, 2005a]. In comparison, intermediate water table during DOY 235–264 in 2004 (Figure 4) maintained capillary rise and higher θ in the upper peat (Figure 5a).

[46] The macroporous structure of the fibric peat favored rapid diffusive O_2 transport in the model from the atmosphere (equations (D1a)–(D1c)) through large air-filled porosities (Figure 5a) with high gaseous diffusivity (equations (D2a)–(D2c)). Thus, during respiration the aqueous O_2 modeled in the thin water films around peat fibers was rapidly replenished by O_2 transferred from the soil gaseous phase (equation (D5)). Greater water retention below 35 cm (Figure 5a) limited the increase of air-filled porosities with WT drawdowns. Thus, modeled O_2 transport depended mainly on a considerably lower aqueous O_2 diffusivity (equations (D4a)–(D4c)), which together with rapid O_2 consumption, caused low aqueous O_2 concentrations to be modeled in deep waterlogged peat (equations (D3a)–(D3c)). These low aqueous O_2 concentrations at depth were sustained by lower transport rates due to low diffusivity in the aqueous phase, and low diffusivity and dissolution from a more constricted gasous phase. Experimental findings for other peatlands confirmed that the unsaturated hemic and upper sapric peat layers (40–60 cm depth range) were likely not well oxygenated even with a deep water table [*Nazaroff*, 1992].

6.2. Reconciling Reported Effects of WT Depth on Respiration in Peatlands

[47] Macroporosity, thickness of fibric peat and natural range of WT variation may help to explain the diverse hydrological effects on bog soil respiration and ecosystem respiration reported in the literature (section 1.1) through manifestation or lack of the respiration offsetting mechanism modeled here. However, a lack of measurements of macropore fractions, depth of the fibric peat, CO_2 production rates and θ of near-surface peat (0–10 cm) for most of the peatlands prevents robust support of the model findings and makes the suggested explanation only hypothetical at this stage.

[48] Increased soil respiration with WT drawdown from 10 cm to 50–60 cm depth below the peat surface observed by *Moore and Dalva* [1993] could be due to shallower fibric peat on the top of their experimental columns, compared to the fibric peat in Mer Bleue hummocks. These columns were assembled in PVC tubes and contained near-surface peat samples from 0–25 cm depth, followed by deep peat samples from 30–60 cm depth. Samples were retrieved from soil profiles in an open bog in Ontario, a poor fen and a treed swamp in Quebec. The top 25 cm of peat in the PVC tubes would remain hydrated through capilliary rise from the deep peat below, with possibly negligible macroporosity and high water retention. Thus, the upward water flux would prevent desiccation of the upper 25 cm of peat in the PVC tubes in a similar way that the fibric peat in Mer Bleue hummocks below the zone of near-surface desiccation, i.e., between 10 cm and 35 cm depths, remained well hydrated from the deep peat below, even with a water table as deep as ~60–70 cm depth (Figures 4 and 5a). In this case, with shallow fibric peat and no near-surface desiccation, soil respiration would rise with WT decline and improved aeration at depth. This is similar to the soil respiration response to WT decline in hollows as modeled in our study.

[49] *Silvola et al.* [1996a] reported an initial increase and subsequent leveling off of peat respiration with WT decline from the peat surface to ~30–40 cm depth below (no details about peatlands' microtopography) in bogs and fens in boreal Finland. This finding could also be attributed to an offsetting mechanism, in which case the water table close to the peatland surface would suppress aerobic respiration and WT drawdown would increase aeration and subsequently respiration. However, as the water table approached ~30–40 cm depth, the near-surface drying would offset increased respiration at depth, which would result in little change in peat respiration with WT drawdown. *Silvola et al.* [1996a] reported further that when the WT dropped below the 30–40 cm depth respiration declined slightly, which might have been due to deepening of the zone of near-surface desiccation, thus limiting respiration in the upper peat profile even more.

[50] Increased ecosystem respiration with WT drawdown to ~20–35 cm depth in a minerotrophic shrub peatland in central Wisconsin observed by *Sulman et al.* [2009] could be caused by initially increased aeration at depth within the sapric peat of high water retention that occupied the soil profile from the top surface down to the sand base at ~50 cm

Table 3. Sensitivity of Simulated Soil Respiration in Hummocks, Hollows, and Total, and Ecosystem Respiration at Mer Bleue Bog During the Growing Season (Mid June to Mid September), Year 2001, to Various Drainage Boundaries, Expressed Through the Minimum Depths of Water Table Variation Maintained in the Model, and Various Microtopography With Different Hummock:Hollow Surface Area Ratios[a]

	Respiration During the Growing Season, Year 2001 (g C m^{-2})					
	Min WT = 40 cm		Min WT = 70 cm		Min WT = 100 cm	
Respiration Component	hmk	hlw	hmk	hlw	hmk	hlw
Fibric peat, vulnerable to desiccation (0–5 cm in hummocks only)[b]	28		21		8	
Fibric peat, less vulnerable to desiccation (>5 cm in hummocks, in hollows)	62	5	70	8	75	20
Hemic and upper sapric peat (down to 100 cm, in hummocks and hollows)	9	29	13	34	23	40
Deeper sapric peat (>100 cm, in hummocks and hollows)	2	2	2	2	2	2
Entire peat depth	101	36	106	44	108	62
Total soil respiration, hummock: hollow surface area ratio 7:3	82 (94%)[c]		87 (100%)[c]		94 (108%)[c]	
Ecosystem respiration, hummock: hollow surface area ratio 7:3	272 (102%)[c]		266 (100%)[c]		263 (99%)[c]	
Total soil respiration, hummock: hollow surface area ratio 1:1	69 (92%)[c]		75 (100%)[c]		85 (113%)[c]	
Ecosystem respiration, hummock: hollow surface area ratio 1:1	245 (101%)[c]		242 (100%)[c]		244 (101%)[c]	
Total soil respiration, hummock: hollow surface area ratio 3:7	56 (89%)[c]		63 (100%)[c]		76 (121%)[c]	
Ecosystem respiration, hummock: hollow surface area ratio 3:7	217 (99%)[c]		219 (100%)[c]		226 (103%)[c]	

[a]Here hmk, hummocks; hlw, hollows; min WT, minimum depths of water table variation.
[b]The hummock surface is the main reference of 0 cm; the hollow surface is referred as 25 cm below the hummock surface.
[c]The values refer to the entire bog.

depth. However, further WT decline was found to have little effect on the ecosystem respiration, which could be due to some limited oxygenation of the sapric peat with a water table falling further down [*Nazaroff*, 1992].

[51] Lack of response of ecosystem respiration to WT drawdown in the wet peat profiles of a patterned sedge fen and a raised *Sphagnum* bog in Minnesota observed by *Updegraff et al.* [2001] could be possibly due to the shallow water table and small WT variation in their experiment. The water table was drawn down only to ~20 cm below the hollow surface (hummock heght above the hollow surface not given).

[52] Lack of response of soil and ecosystem respiration to WT drawdowns in dry peatlands, such as Mer Bleue bog [*Blodau et al.*, 2007; *Lafleur et al.*, 2005a; *Moore et al.*, 2003], could be due to a water table varying deep in the peat profile, but over a narrow range of depth. This could result in the highest respiration rates occurring at some intermediate WT depth. However, these rates would not significantly differ from the respiration rates at higher or lower WT depths, given that the water table does not vary considerably (i.e., ±20 cm) from its intermediate position. If the water table varied over a wider range of depth in the peat profle, the highest respiration rates at an intermediate WT depth could significantly differ from those at rather high WT depths and waterlogged peat, and at rather low WT depths and severely dry peat. In this case, decrease of soil and ecosystem respiration with WT above or below an optimum depth, could be due to suppressing the aerobic respiration through waterlogging, or suppressing the near-surface microbial activity through desiccation.

[53] To explore sensitivity of respiration offset under different drainage boundaries and microtopography, we compared simulated soil and ecosystem respiration with WT variation down to 40 cm, 70 cm (Mer Bleue bog) and 100 cm, and with different hummock: hollow surface area ratios of 7:3 (Mer Bleue bog), 1:1 and 3:7 (Table 3). Soil respiration in hummocks remained highly conservative with all the mimimum depths of WT variation, as increase of respiration at depth was offset by decrease of nearsurface soil respiration. The slight tendency to increase with min WT of 100 cm was due to slightly faster deepening of aeration at depth compared to deepening of nearsurface desiccation. In hollows soil respiration with min WT of 100 cm was almost twice that with min WT of 40 cm. However, the soil and ecosystem respiration with hummock: hollow surface area ratio of 7:3, as is at Mer Bleue bog, remained conservative mainly due to decrease of moss respiration at hummocks, which was 225% with min WT of 40 cm and 44% with min WT of 100 cm from that with min WT of 70 cm. Although the soil respiration increased with deeper WT variation and increase of the hollow surface area, the ecosystem respiration remained highly conservative with WT variation down to 40 cm, 70 cm and 100 cm for each hummock: hollow surface area ratio (Table 3) due to decrease of moss respiration at hummocks.

6.3. Implications for Potential Climate Change Effects on Bog Ecosystem Respiration

[54] The hypothesized respiration offset modeled here is expected to result in different responses of respiration to the water table in different peatlands, depending on the range of WT variation and the thickness of macroporous fibric peat that determines θ in the upper peat profile. "Wet" peatlands with high WT would be expected to start emitting larger CO_2 fluxes with WT drawdowns and increasing aeration at depth, as long as the surface doesn't desiccate. Once near-surface drying takes place, CO_2 emissions would change little with further lowering of the water table. Lowering the water table in "dry" peatlands, such as Mer Bleue bog, might cause either little change or a slow increase of CO_2 emissions, arising mostly from deep and less productive peat. The former scenario might occur if declines in respiration from deepening near-surface desiccation offset rises in respiration from increased aeration in deep peat with WT drawdown. The latter scenario might occur if the water table dropped more rapidly than did the near-surface desiccation, so that the respiration offset was incomplete.

[55] Thus, our findings still support the widely held view that global warming would increase respiration in peatlands by decreasing peat θ and lowering the water table [*Moore et al.*, 1998]. However, the magnitude of the respiration increase might vary among different peatlands and would depend on balancing the decrease of CO_2 emissions from the upper peat caused by near-surface desiccation and the increase of CO_2 emissions from the deeper peat caused by increased aeration. Therefore, with minimal dependence of ecosystem respiration on subsurface hydrology, gross primary productivity may become the main determinant of net ecosystem productivity in peatlands with varying water table depths, which is in the main focus of another study that builds upon the findings of this research.

7. Conclusions

[56] The findings of this study suggest that reduced near-surface microbial respiration with WT drawdowns offsets increased root and microbial respiration in aerated peat below the zone of near-surface desiccation. This is referred to here as the respiration offsetting mechanism, which is manifested mainly in peat hummocks. A conservative response of bog ER to WT drawdowns was further determined by offsetting increased soil respiration in hollows by decreased aboveground respiration of drying moss on hummocks. Depending on the range of WT variation within the peat profile and the thickness of macroporous fibric peat that determines moisture content at near surface, the strength of the respiration offsetting mechanism might vary among different peatlands, thus suggesting an explanation for some of the contradictory findings reported in the literature on hydrological effects on ecosystem respiration and its components. This mechanism also has implications for peatland response to future climate change.

Appendix A: Hydrolysis, Microbial Respiration, and Microbial Growth

A1. Exoenzyme Hydrolysis Driven by Active Heterotrophic Microbial Biomass

[57]

$$D_{Si,j,C} = \sum_n M_{i,n,a} f_{tg} \{ D_{Sj,C}[S_{i,C}] \} / \{ [S_{i,C}] + K_D \cdot (1.0 + [\sum_n M_{i,n,a}]/K_{iD}) \} \qquad [S_{i,C}] = \sum_j [S_{i,j,C}] \tag{A1a}$$

$$D_{Bi,j,C} = \sum_n M_{i,n,a} f_{tg} \{ D_{Sj,B}[S_{i,B}] \} / \{ [S_{i,B}] + K_D \cdot (1.0 + [\sum_n M_{i,n,a}]/K_{iD}) \} \qquad [S_{i,B}] = \sum_j [S_{i,j,B}] \tag{A1b}$$

$$D_{Zi,j,C} = \sum_n M_{i,n,a} f_{tg} \{ D_{Zj,C}[Z_{i,C}] \} / \{ [Z_{i,C}] + K_D \cdot (1.0 + [\sum_n M_{i,n,a}]/K_{iD}) \} \qquad [Z_{i,C}] = \sum_j [Z_{i,j,C}] \tag{A1c}$$

$$\left[\sum_n M_{i,n,a}\right] = M_{i,n,a}/\theta_l \qquad \text{soil layer } l \tag{A2}$$

A2. Microbial Respiration ($R_{hi,n} = R_{hi,e} + R_{hi,d} + R_{hi,f} + R_{hi,m}$)

A2.1. Heterotrophic Obligate Aerobes and Facultative Anaerobes: Denitrifies (Aerobic Reactions) (*e*)

[58] Aerobic respiration ($n = e$): $DOC + O_2 \rightarrow CO_2 + H_2O$.

$$R_{hi,e} = R'_e M_{i,e,a} f_{tg} f_{NP} ([Q_{i,C}]/([Q_{i,C}] + K_{QC})) \cdot (U_{O2i,e}/U'_{O2i,e}) \qquad \text{respiration constrained by } Tl,\ N,\ P,\ [Q_{i,C}],\ O_2 \text{ uptake : to equation (B2)} \tag{A3}$$

$$U'_{O2i,e} = \{ R'_e M_{i,e,a} f_{tg} f_{NP} ([Q_{i,C}]/([Q_{i,C}] + K_{QC})) \}/RQ_{O2} \qquad O_2 \text{ uptake with nonlimiting } O_2 (O_2 \text{ demand}) \tag{A4}$$

$$U_{O2i,e} = U'_{O2i,e} \{ [O_{2mi,e}]/([O_{2mi,e}] + K_{O2}) \} \qquad O_2 \text{ uptake with ambient } O_2 \text{ (constrained by } O_2 \text{ supply)} \tag{A5a}$$

$$= 4\pi n\, M_{i,e,a}\, \sigma_{O2AS} [r_m r_w/(r_w - r_m)] \cdot ([O_{2AS}] - [O_{2mi,e}]) \qquad U_{O2i,e} \text{ solved through } [O_{2mi,e}] \text{ from } [O_{2AS}] \text{ and } \sigma_{O_{2AS}} \tag{A5b}$$

$$Y_e = -\Delta G'_{O2}/E_m \qquad \text{microbial biomass yield (heterotrophic aerobes)} \tag{A6}$$

A2.2. Heterotrophic Facultative Anaerobes: Denitrifiers (Anaerobic Reactions) (*d*)

[59] Anaerobic respiration ($n = d$): $DOC + NO_3 \rightarrow NO_2 \rightarrow N_2O \rightarrow N_2 + CO_2 + H_2O$.

$$R_{hi,d} = R_{hi,d\ NO3} + R_{hi,d\ NO2} + R_{hi,d\ N2O} \qquad NO_x - \text{constrained denitrifier total anaerobic respiration} \tag{A7}$$

$$Y_d = -\Delta G'_d/E_m \qquad \text{microbial biomass yield (anaerobic denitrifiers)} \tag{A8}$$

A2.3. Heterotrophic Obligate Anaerobes: Fermenters and H_2-Producing Acetogens (Syntrophs) (*f*)

[60] Fermentation ($n = f$): $DOC \rightarrow 0.67A_{i,C} + 0.33CO_2 + 0.11H_2$

$$R_{hi,f} = R'_f M_{i,f,a} f_{tg} f_{NP} \{ [Q_{i,C}]/([Qi,C] + K_f \cdot (1 + [O_{2AS}]K_{iO2})) \} \qquad \text{fermentation inhibited by aqueous } O_2 \tag{A9}$$

$$Y_f = -\Delta G_f/E_m \qquad \text{microbial biomass yield (fermenters and acetogens} - \text{syntrophs)} \tag{A10a}$$

$$\Delta G_f = f(\Delta G'_f, [H_2], R, T_S) \qquad \begin{array}{l} H_2 - regulated\ syntrophy \\ between\ H_2\ producers\ and \\ H_2\ consumers \end{array} \tag{A10b}$$

A2.4. Heterotrophic Obligate Anaerobes: Acetotrophic Methanogens (*m*)

[61] Anaerobic respiration ($n = m$): Acetate→ $0.5CH_4 + 0.5CO_2$.

$$R_{hi,m} = R'_m\, M_{i,m,a}\, f_{tg} f_{NP}\, \left\{ [A_{i,C}] / \left([A_{i,C}] + K_m \right) \right\} \tag{A11}$$

$$Y_m = -\Delta G'_m / E_m \qquad \begin{array}{l} microbial\ biomass\ yield \\ (heterotrophic \\ methanogens) \end{array} \tag{A12}$$

A3. Partitioning of the Microbial CO_2 Production Among Maintenance and Growth Respiration, Microbial Uptake of Organic C, Death and Growth, Active Microbial Biomass

[62]

$$R_{mi,n,j} = R_m M_{i,n,j,N} f_{tm} \qquad R_{hi,n} \in \{R_{hi,e};\ R_{hi,d};\ R_{hi,f};\ R_{hi,m}\} \tag{A13}$$

$$R_{gi,n} = R_{hi,n} - \sum\nolimits_j R_{mq,j} \tag{A14}$$

$$U_{i,n} = \left\{ \left[\sum\nolimits_j R_{mi,n,j} + R_{gi,n}(1 - Y_n) \right]; R_{gi,n} \right\} \qquad Y_n \in \{Y_e;\ Y_d;\ Y_f;\ Y_m\} \tag{A15}$$

$$D_{Mi,n,j,C} = D_{Mi,n,j} M_{i,n,j,C} f_{tg} \tag{A16}$$

$$\delta M_{i,n,j,C}/\delta t = \begin{array}{l} \{(F_j U_{i,n} - F_j R_{hi,n} - D_{Mi,n,j,C});\ \{[R_{hi,n} > R_{mi,n,j}];\ [R_{hi,n} < \\ (F_j U_{i,n} - R_{mi,n,j} - D_{Mi,n,j,C})\} \qquad R_{mi,n,j}]\} \end{array} \tag{A17}$$

$$M_{i,n,a,C} = M_{i,n,l,C} + M_{i,n,r,C} F_r / F_l \qquad \begin{array}{l} active\ heterotrophic \\ microbial\ biomass, \\ j = \{l; r\} \end{array} \tag{A18}$$

Appendix B: Autotrophic Belowground Plant Respiration (Under Ambient O_2)

[63]

$$R_{a,P} = \sum\nolimits_i \sum\nolimits_l \sum\nolimits_z (R_{ci,l,z} + R_{si,l,z}) \qquad \begin{array}{l} i\ is\ plant\ population;\ l\ is \\ soil\ layer;\ z\ is\ root\ axis \end{array} \tag{B1}$$

$$R_{mi,l,z} = N_{i,l,z} R'_{mp} f_{tmi} \tag{B2}$$

$$R_{ci,l,z} = R'_c \varsigma_{\ ci,l,z} f_{tai} f_{Nai} \left(U_{O2i,l,z} / U'_{O2i,l,z} \right) \tag{B3}$$

$$U'_{O2i,l,z} = R_{a,P} / RQ_{O2} \qquad \begin{array}{l} root\ O_2\ uptake\ with \\ nonlimiting\ O_2 \\ (O_2\ demand) \end{array} \tag{B4}$$

$$U_{O2i,l,z} = U'_{O2i,l,z} \{ [O_{2ARi,l,z}] / ([O_{2ARi,l,z}] + K_{O2}) \} \qquad root\ O_2\ uptake\ with\ ambient\ O_2 (constrained\ by\ O_2\ supply) \tag{B5a}$$

$$= -U_{i,l,z}[O_{2AS,l}] + 2\pi L_{i,l,z} \sigma_{O2UR} ([O_{2AS,l}] - [O_{2ARi,l,z}]) / ln((r_{Si,l,z} + r_W)/r_{Si,l,z}) \qquad \begin{array}{l} U_{O2i,l,z}\ solved\ through \\ [O_{2ARi,l,z}]\ from\ [O_{2AS,l}]\ and \\ \sigma_{O2AS,l} \end{array} \tag{B5b}$$

$$= 2\pi L_{i,l,z} \sigma_{O2UR} ([O_{2APi,l,z}] - [O_{2ARi,l,z}]) / (r_{Si,l,z}/r_{Pi,l,z}) \tag{B5c}$$

$$R_{gi,l,z} = (R_{ci,l,z} - R_{mi,l,z}) f(\psi_{t\ i,l,z} - \psi_t) \tag{B6}$$

$$\delta M_{Ri,l,z}/\delta_t = U_{Ri,l,z}(R_{gi,l,z}, R_{mi,l,z}) - R_{gi,l,z} - R_{mi,l,z} - D_{Ri,l,z} \tag{B7}$$

Appendix C: Autotrophic Aboveground Plant Respiration (Under Nonlimiting O_2)

[64]

$$R_{a,A} = \sum\nolimits_i \sum\nolimits_j \sum\nolimits_z (R_{ci,j,z} + R_{si,j,z}) \qquad i\ is\ plant\ population;\ j\ is\ branch;\ z\ is\ plant\ organ \tag{C1}$$

$$R_{ci,j,z} = R'_c \varsigma_{\ ci,j,z} f_{tai} f_{Nai} \tag{C2}$$

$$R_{si,j,z} = \{(R_{mi,j,z} - R_{ci,j,z}); 0\} \qquad \{[R_{ci,j,z} < R_{mi,j,z}];\ [R_{ci,j,z} > R_{mi,j,z}]\} \tag{C3}$$

$$R_{mi,j,z} = N_{i,j,z} R'_{mp} f_{tmi} \tag{C4}$$

Appendix D: Transport and Transfer of O_2 ($\gamma = O_2$), and Other Gases and Inorganic Solutes (γ) From the Atmosphere to the Soil Surface, and Through the Soil

D1. Convective-Dispersive Transport of O_2 ($\gamma = O_2$) and Other Gases (γ) in the Gaseous Phase of the Soil

[65]

$$Q_{\gamma_{GS},x(x,y,z)} = Q_{w,x(x,y,z)} [\gamma_{GS}]_{(x,y,z)} + 2\sigma_{\gamma_{GS},x(x,y,z)} \cdot \left([\gamma_{GS}]_{(x,y,z)} - [\gamma_{GS}]_{(x+1,y,z)} \right) / \left(l_{x(x+1,y,z)} + l_{x(x,y,z)} \right) \tag{D1a}$$

$$Q_{\gamma_{GS},y(x,y,z)} = Q_{w,y(x,y,z)}[\gamma_{GS}]_{(x,y,z)} + 2\sigma_{\gamma_{GS},y(x,y,z)} \cdot \left([\gamma_{GS}]_{(x,y,z)} - [\gamma_{GS}]_{(x,y+1,z)}\right) / \left(l_{y(x,y+1,z)} + l_{y(x,y,z)}\right) \quad \text{(D1b)}$$

$$Q_{\gamma_{GS},z(x,y,z)} = Q_{w,z(x,y,z)}[\gamma_{GS}]_{(x,y,z)} + 2\sigma_{\gamma_{GS},z(x,y,z)} \cdot \left([\gamma_{GS}]_{(x,y,z)} - [\gamma_{GS}]_{(x,y,z+1)}\right) / \left(l_{z(x,y,z+1)} + l_{z(x,y,z)}\right) \quad \text{(D1c)}$$

$$\sigma_{\gamma GS,x(x,y,z)} = \sigma'_{\gamma GS} f_{t\sigma G(x,y,z)} \left[0.5\left(\varepsilon_{a(x,y,z)} + \varepsilon_{a(x+1,y,z)}\right)\right]^{vg} / \varepsilon^2_{t(x,y,z)} \qquad \sigma'_{\gamma GS} = \sigma'_{O2G} \quad \text{(D2a)}$$

$$\sigma_{\gamma GS,y(x,y,z)} = \sigma'_{\gamma GS} f_{t\sigma G(x,y,z)} \left[0.5\left(\varepsilon_{a(x,y,z)} + \varepsilon_{a(x,y+1,z)}\right)\right]^{vg} / \varepsilon^2_{t(x,y,z)} \qquad \sigma'_{\gamma GS} = \sigma'_{O2G} \quad \text{(D2b)}$$

$$\sigma_{\gamma GS,z(x,y,z)} = \sigma'_{\gamma GS} f_{t\sigma G(x,y,z)} \left[0.5\left(\varepsilon_{a(x,y,z)} + \varepsilon_{a(x,y,z+1)}\right)\right]^{vg} / \varepsilon^2_{t(x,y,z)} \qquad \sigma'_{\gamma GS} = \sigma'_{O2G} \quad \text{(D2c)}$$

D2. Convective-Dispersive Transport of O_2 ($\gamma = O_2$), and Other Gases and Inorganic Solutes (γ) Within the Aqueous Phase of the Soil

[66]

$$Q_{\gamma AS,x(x,y,z)} = Q_{w,x(x,y,z)}[\gamma_{AS}]_{(x,y,z)} + 2\sigma_{\gamma AS,x(x,y,z)} \cdot \left([\gamma_{AS}]_{(x,y,z)} - [\gamma_{AS}]_{(x+1,y,z)}\right) / \left(l_{x(x+1,y,z)} + l_{x(x,y,z)}\right) \quad \text{(D3a)}$$

$$Q_{\gamma AS,y(x,y,z)} = Q_{w,y(x,y,z)}[\gamma_{AS}]_{(x,y,z)} + 2\sigma_{\gamma AS,y(x,y,z)} \cdot \left([\gamma_{AS}]_{(x,y,z)} - [\gamma_{AS}]_{(x,y+1,z)}\right) / \left(l_{y(x,y+1,z)} + l_{y(x,y,z)}\right) \quad \text{(D3b)}$$

$$Q_{\gamma AS,z(x,y,z)} = Q_{w,z(x,y,z)}[\gamma_{AS}]_{(x,y,z)} + 2\sigma_{\gamma AS,z(x,y,z)} \cdot \left([\gamma_{AS}]_{(x,y,z)} - [\gamma_{AS}]_{(x,y,z+1)}\right) / \left(l_{z(x,y,z+1)} + l_{z(x,y,z)}\right) \quad \text{(D3c)}$$

$$\sigma_{\gamma AS,x(x,y,z)} = \lambda|Q_{w,x(x,y,z)}| + \sigma'_{\gamma AS} f_{t\sigma A\ (x,y,z)} \tau_{AS(x,y,z)} 0.5\left(\varepsilon_{w(x,y,z)} + \varepsilon_{w(x+1,y,z)}\right) \qquad \sigma'_{\gamma AS} = \sigma'_{O2A} \quad \text{(D4a)}$$

$$\sigma_{\gamma AS,y(x,y,z)} = \lambda|Q_{w,y(x,y,z)}| + \sigma'_{\gamma AS} f_{t\sigma A\ (x,y,z)} \tau_{AS(x,y,z)} 0.5\left(\varepsilon_{w(x,y,z)} + \varepsilon_{w(x,y+1,z)}\right) \qquad \sigma'_{\gamma AS} = \sigma'_{O2A} \quad \text{(D4b)}$$

$$\sigma_{\gamma AS,z(x,y,z)} = \lambda|Q_{w,z(x,y,z)}| + \sigma'_{\gamma AS} f_{t\sigma A\ (x,y,z)} \tau_{AS(x,y,z)} 0.5\left(\varepsilon_{w(x,y,z)} + \varepsilon_{w(x,y,z+1)}\right) \qquad \sigma'_{\gamma AS} = \sigma'_{O2A} \quad \text{(D4c)}$$

$$\sigma_{\gamma AS(x,y,z)} = \lambda|Qw,z(x,y,z)| + \sigma'_{\gamma AS} f_{t\sigma A\ (x,y,z)} \tau_{AS(x,y,z)} \varepsilon_{w(x,y,z)} \qquad \sigma'_{\gamma AS} = \sigma'_{O2A}, \gamma = O_2 : \sigma_{\gamma AS(x,y,z)} = \sigma_{O2AS\ (x,y,z)} \quad \text{(D4d)}$$

D3. Volutilization-Dissolution Transfer of O_2 ($\gamma = O_2$) and Other Gases (γ) Between Gaseous and Aqueous Phases of the Soil

[67]

$$T_{\gamma S\ (x,y,z)} = a_{S(x,y,z)} \sigma_{\gamma t} \left(\mathbf{S}'_{\gamma} f_{tS\gamma(x,y,z)} [\gamma_{GS}]_{(x,y,z)} - [\gamma_{AS}]_{(x,y,z)}\right) \qquad S'_{\gamma} = S'_{O2} \quad \text{(D5)}$$

Appendix E: Transport and Transfer of O_2 in Roots

[68]

$$Q_{O2GPi,l,z} = \sigma_{O2\ GPi,l,z}\left([O_{2A}] - [O_{2GPi,l,z}]\right) A_{Pi,l,z} / z_{Pi,l,z}$$

i is plant population; l is soil layer; z is root axis (E1)

$$\sigma_{O2\ GPi,l,z} = \sigma'_{O2GS} f_{t\sigma O2G\ i,l,z} \theta_P^{vp} \quad \text{(E2)}$$

$$T_{O2\ Pi,l,,z} = a_{Pi,l,z} \sigma_{\gamma t} \left(S'_{O2} f_{tO2P\ i,l,z} [O_{2GPi,l,z}] - [O_{2APi,l,z}]\right) \quad \text{(E3)}$$

Notation

Indexes, associated with relevant model equations (Appendices A–E)

- *d* facultative anaerobes, i.e., denitrifiers.
- *e* obligate aerobes.
- *f* fermenters and acetogens.
- *h* heterotrophs.
- *i* organic matter-microbe complex.
- *j* structural (labile or resistant) or kinetic (carbohydrate, protein, cellulose or lignin) component; branch index.
- *k* elemental fractions of C, N and P.
- *l* labile structural component; soil layer.
- *m* obligate anaerobes, i.e., methanogens.
- *n* the number of all heterotrophic microbial populations.
- *r* resistant structural component.
- *x* horizontal direction and coordinate of a landscape position.
- *y* horizontal direction and coordinate of a landscape position.
- *z* vertical direction and coordinate of a landscape position; index for primary *(z = 1)* and secondary *(z = 2)* root and mycorrhizal axes; index for aboveground plant organs.

Model variables, associated with relevant model equations (Appendices A–E)

$A_{Pi,l,z}$ root cross-sectional area of ith plant population, lth soil layer, zth root axis (equation (E1)), $m^2\ m^{-2}$.

$[A_{i,c}]$ aqueous acetate concentration associated with ith organic matter-microbe complex, g C m^{-3}.

$D_{Mi,n,j,C}$ decomposition rate of dead microbial carbon of nth microbial population, ith organic matter-microbe complex, jth structural component (equations (A16) and (A17)), g C $m^{-2}\ h^{-1}$.

$D_{Ri,l,z}$ root litterfall of ith plant population, lth soil layer, zth root axis (equation (B7)), g C $m^{-2}\ h^{-1}$.

$D_{Si,j,C}$ rate of hydrolysis of solid organic matter, ith organic matter-microbe complex, jth kinetic component (equation (A1a)), g C $m^{-2}\ h^{-1}$.

$D_{Bi,j,C}$ rate of hydrolysis of sorbed organic matter, ith organic matter-microbe complex, jth kinetic component (equation (A1b)), g C $m^{-2}\ h^{-1}$.

$D_{Zi,j,C}$ rate of hydrolysis of microbial residues, ith organic matter-microbe complex, jth structural component (equation (A1c)), g C $m^{-2}\ h^{-1}$.

F_j labile ($j = l$) or resistant ($j = r$) component of microbial biomass (equations (A17) and (A18)), dimensionless.

$\Delta G'_n$ microbial energy yield of nth microbial population (equation (A6)) with $n = e$, equation (A8) with $n = d$, equation (A10a) with $n = f$, equation (A12) with $n = m$), kJ g C^{-1}.

$[H_2]$ aqueous hydrogen concentration in soil (equation (A10b), where f means a function), g H m^{-3}.

$L_{i,l,z}$ root length of ith plant population, lth soil layer, zth root axis (equations (B5b) and (B5c)), m m^{-2}.

M microbial biomass, g C m^{-2}.

$M_{i,n,a}$ active microbial biomass of the nth microbial population, associated with ith organic matter-microbe complex (equations (A1a)–(A1c) and (A2), equations (A3) and (A4) with $n = e$, equation (A9) with $n = f$, and equation (A11) with $n = m$), g C m^{-2}.

$[M_{i,n,a}]$ aqueous concentration of $M_{i,n,a}$ (equations (A1a)–(A1c) and (A2)), g C m^{-3}.

$M_{i,n,a,C}$ microbial carbon of $M_{i,n,a}$ (equation (A18)), g C m^{-2}.

$M_{i,n,j,C}$ carbon content of the total microbial biomass of nth microbial population, associated with ith organic matter-microbe complex, jth structural component (equation (A17)), g C m^{-2}.

$\delta M_{i,n,j,C}$ change of $M_{i,n,j,C}$ per a model time step δt (equation (A17)), g C m^{-2}.

$M_{i,n,l,C}$ labile ($j = l$) fraction of $M_{i,n,j,C}$ (equation (A17)), g C m^{-2}.

$M_{i,n,r,C}$ resistant ($j = r$) fraction of $M_{i,n,j,C}$ (equation (A17)), g C m^{-2}.

$M_{i,n,j,N}$ nitrogen content of the total microbial biomass of nth microbial population, associated with ith organic matter-microbe complex, jth structural component (equation (A13)), g N m^{-2}.

$M_{Ri,l,z}$ root biomass of ith plant population, lth soil layer, zth root axis (equation (B7)), g C $m^{-2}\ h^{-1}$.

$\delta M_{Ri,l,z}$ change of $M_{Ri,l,z}$ per a model time step δt (equation (B7)), g C m^{-2}.

$N_{i,j,z}$ nitrogen content of ith plant population, jth branch, zth aboveground plant organ (equation (C4)), g N m^{-2}.

$N_{i,l,z}$ root nitrogen content of ith plant population, lth soil layer, zth root axis (equation (B2)), g N m^{-2}.

$[O_{2A}]$ concentration of O_2 in the atmosphere (equation (E1)), g O m^{-3}.

$[O_{2APi,l,z}]$ concentration of O_2 in root aqueous phase of ith plant population, lth soil layer, zth root axis (equations (B5c) and (E3)), g O m^{-3}.

$[O_{2ARi,l,z}]$ aqueous O_2 concentrations at respiratory sites on root and myccorhizal surfaces of ith plant population, lth soil layer, zth root axis (equations (B5a)–(B5c)), g O m^{-3}.

$[O_{2AS}]$ aqueous O_2 concentration in soil (equation (A5b)), associated with lth soil layer (equation (B5b)), g O m^{-3}.

$[O_{2GPi,l,z}]$ concentration of O_2 in root gaseous phase of ith plant population, lth soil layer, zth root axis (equations (E1) and (E3)), g O m^{-3}.

$[O_{2mi,e}]$ ambient aqueous O_2 concentrations at microbial microsites (equations (A5a) and (A5b)), g O m^{-3}.

$[Q_{i,c}]$ concentration of C hydrolysis products (equations (A3), (A4), and (A9)), g C m^{-3}.

$Q_{O2GPi,l,z}$ transport of O_2 from the atmosphere through plant root axes, ith plant population, lth soil layer, zth root axis (equation (E1)), g O $m^{-2}\ h^{-1}$.

Q_w subsurface water flux at a given model cell (x,y,z) in a given horizontal x, y or vertical z direction (equations (D1a)–(D1c), (D3a)–(D3c), and (D4a)–(D4d)), $m^3\ m^{-2}\ h^{-1}$.

$Q\gamma_{AS}$ transport of gas/solute γ through the aqueous phase of the soil at a given model cell (x,y,z) in a given horizontal x, y or vertical z direction (equations (D3a)–(D3c)), g $m^{-2}\ h^{-1}$.

$Q\gamma_{GS}$ transport of gas γ through the gaseous phase of the soil at a given model cell (x,y,z) in a given horizontal x, y or vertical z direction (equations (D1a)–(D1c)), g $m^{-2}\ h^{-1}$.

$R_{a,A}$ total autotrophic aboveground respiration (equation (C1)), g C $m^{-2}\ h^{-1}$.

$R_{a,P}$ total root respiration (equation (B1)), g C $m^{-2}\ h^{-1}$.

$R_{ci,j,z}$ respiration of nonstructural carbon of the ith plant population, jth branch, zth aboveground plant organ (equations (C1)–(C3)), g C $m^{-2}\ h^{-1}$.

$R_{ci,l,z}$ respiration of root nonstructural carbon of the *i*th plant population, *l*th soil layer, *z*th root axis (equations (B1), (B3), and (B6)), g C m^{-2} h^{-1}.

$R_{gi,l,z}$ root growth respiration of the *i*th plant population, *l*th soil layer, *z*th root axis (equations (B6) and (B7)), g C m^{-2} h^{-1}.

$R_{gi,n}$ microbial growth respiration of the *n*th microbial population, *i*th organic matter-microbe complex (equations (A14) and (A15)), g C m^{-2} h^{-1}.

$R_{hi,d}$ facultative anaerobic respiration of denitrifiers of the *i*th organic matter-microbe complex (equation (A7)), g C m^{-2} h^{-1}.

$R_{hi,e}$ microbial aerobic respiration of the *i*th organic matter-microbe complex (equation (A3)), g C m^{-2} h^{-1}.

$R_{hi,f}$ fermentation-produced CO_2 by fermenters and acetogens of the *i*th organic matter-microbe complex (equation (A9)), g C m^{-2} h^{-1}.

$R_{hi,m}$ anaerobic respiration of obligate anaerobes, i.e., acetotrophic methanogens, of the *i*th organic matter-microbe complex (equation (A11)), g C m^{-2} h^{-1}.

$R_{hi,n}$ heterotrophic microbial respiration of the *n*th microbial population, *i*th organic matter-microbe complex (equations (A14) and (A17)), g C m^{-2} h^{-1}.

$R_{hi,dNO3}$ NO_3^-constrained respiration of the *i*th organic matter denitrifier complex (equation (A7)), g C m^{-2} h^{-1}.

$R_{hi,dNO2}$ NO_2^-constrained respiration of the *i*th organic matter denitrifier complex (equation (A7)), g C m^{-2} h^{-1}.

$R_{hi,dN2O}$ N_2O-constrained respiration of the *i*th organic matter denitrifier complex (equation (A7)), g C m^{-2} h^{-1}.

$R_{mi,j,z}$ maintenance respiration of the *i*th plant population, *j*th branch, *z*th aboveground plant organ (equations (C3) and (C4)), g C m^{-2} h^{-1}.

$R_{mi,n,j}$ microbial maintenance respiration of the *n*th microbial population, *i*th organic matter-microbe complex, *j*th structural component (equations (A13), (A15), and (A17)), g C m^{-2} h^{-1}.

$R_{mi,l,z}$ root maintenance respiration of the *i*th plant population, *l*th soil layer, *z*th root axis (equations (B2), (B6), and (B7)), g C m^{-2} h^{-1}.

$R_{si,j,z}$ respiration of remobilized carbon of the *i*th plant population, *j*th branch, *z*th aboveground plant organ (equations (C1) and (C3)), g C m^{-2} h^{-1}.

$R_{si,l,z}$ respiration of root remobilized carbon of the *i*th plant population, *l*th soil layer, *z*th root axis (equation (B1)), g C m^{-2} h^{-1}.

$[S_{i,C}]$ substrate concentration, for all the components *j* of the *i*th complex of the solid organic matter (equation (A1a)), g C Mg^{-1}.

$[S_{i,B}]$ substrate concentration, for all the components *j* of the *i*th complex of the sorbed organic matter (equation (A1b)), g C Mg^{-1}.

$T_{O2Pi,l,z}$ transfer of O_2 between its gaseous and aqueous phases in roots, *i*th plant population, *l*th soil layer, *z*th root axis (equation (E3)), g O_2 m^{-2} h^{-1}.

$T\gamma_S$ transfer of each gas (oxygen, when $\gamma = O_2$) between soil gaseous (*GS*) and aqueous (*AS*) phases at a given model cell (*x,y,z*) (equation (D5)), g m^{-2} h^{-1}.

$U_{i,l,z}$ root water uptake/exudation of the *i*th plant population, *l*th soil layer, *z*th root axis (equation (B5b)), m^3 m^{-2} h^{-1}.

$U_{i,n}$ microbial uptake of hydrolysis products, acetate, CO_2 and H_2 (equations (A15) and (A17)), g C m^{-2} h^{-1}.

$U_{O2i,e}$ microbial O_2 uptake of the *i*th organic matter-microbe complex under ambient O_2 (equations (A3) and (A5a)), g O m^{-2} h^{-1}.

$U_{O2i,l,z}$ root O_2 uptake under ambient O_2, *i*th plant population, *l*th soil layer, *z*th root axis (equations (B3) and (B5a)), g O m^{-2} h^{-1}.

$U'_{O2i,e}$ microbial O_2 demand of the *i*th organic matter-microbe complex under ambient O_2 (equations (A3), (A4), and (A5a)), g O m^{-2} h^{-1}.

$U'_{O2i,l,z}$ root O_2 demand, *i*th plant population, *l*th soil layer, *z*th root axis (equations (B3), (B4), and (B5a)), g O m^{-2} h^{-1}.

$U_{Ri,l,z}$ root nutrient uptake of the *i*th plant population, *l*th soil layer, *z*th root axis (equation (B7)), g C m^{-2} h^{-1}.

Y_n microbial biomass growth yield of *n*th microbial population (equation (A15), equation (A6) with $n = e$, equation (A8) with $n = d$, equation (A10a) with $n = f$, and equation (A12) with $n = m$), g C g C^{-1}.

$[Z_{i,C}]$ substrate concentration for all the components *j* of the *i*th complex of the microbial residue (equation (A1c)), g C Mg^{-1}.

$a_{Pi,l,z}$ air-water interfacial area in roots, *i*th plant population, *l*th soil layer, *z*th root axis (equation (E3)), m^2 m^{-2}.

a_S air-water interfacial area in soil at a given model cell (*x,y,z*) (equation (D5)), m^2 m^{-2}.

f_{Nai} function for nutrient effects on root respiration of nonstructural carbon (equations (B3) and (C2)), dimensionless.

f_{tai} function for temperature effects on root respiration of nonstructural carbon (equations (B3) and (C2)), dimensionless.

f_{tmi} function for temperature effects on root maintenance respiration (equation (B2)), dimensionless.

f_{NP} function for nutrient (N and P) effects on microbial respiration (equations (A3), (A4)), dimensionless.

$f_{tS\gamma}$ function for temperature effects on solubility of gas γ at a given model cell (*x,y,z*) (equation (D5)), dimensionless.

f_{tg} Arrhenius function for temperature sensitivity (equations (A1a)–(A1c), (A3), (A4), (A9), (A11), and (A16)), dimensionless.

$f_t\sigma_{O2Gi,l,z}$ function for temperature effects on root O_2 gaseous diffusivity of the *i*th plant population, *l*th soil layer, *z*th root axis (equation (E2)), dimensionless.

$f_{tO2Pi,l,z}$ function for temperature effects on O_2 transfer in roots, *i*th plant population, *l*th soil layer, *z*th root axis (equation (E3)), dimensionless.

$f_t\sigma_A$ function for temperature effects on aqueous dispersivity-diffusivity of a given gas γ at a given model cell (*x,y,z*) (equations (D4a)–(D4d)), dimensionless.

$f_t\sigma_G$ function for temperature effects on gaseous dispersivity-diffusivity of a given gas γ at a given model cell (*x,y,z*) (equations (D2a)–(D2c)), dimensionless.

l_x length of a given model cell (*x,y,z*) in horizontal direction *x* (equations (D1a)–(D1c) and (D3a)–(D3c)), m.

l_y length of a given model cell *(x,y,z)* in horizontal direction *y* (equations (D1a)–(D1c) and (D3a)–(D3c)), m.

l_z thickness of a given model cell *(x,y,z)* in vertical direction *z* (equations (D1a)–(D1c) and (D3a)–(D3c)), m.

$r_{Pi,l,z}$ radius of root porous core, *i*th plant population, *l*th soil layer, *z*th root axis (equation (B5c)), m.

$r_{Si,l,z}$ root radius, *i*th plant population, *l*th soil layer, *z*th root axis (equations (B5b) and (B5c)), m.

r_W thickness of the water film at root and myccorhizal surfaces (equations (A5b) and (B5b)), m.

$z_{Pi,l,z}$ root depth from the soil surface, *i*th plant population, *l*th soil layer, *z*th root axis (equation (E1)), m.

$[\gamma_{AS}]$ aqueous concentrations of gas/solute γ in soil water of a given model cell (*x,y,z*) (equations (D3a)–(D3c)), g m^{-3}.

$[\gamma_{GS}]$ gaseous concentration of gas/solute γ in soil water of a given model cell (*x,y,z*) (equations (D1a)–(D1c)), g m^{-3}.

ε_a air-filled soil porosity of a given model cell (*x,y,z*) (equations (D2a)–(D2c)), m^3 m^{-3}.

ε_t total soil porosity of a given model cell (*x,y,z*) (equations (D2a)–(D2c)), m^3 m^{-3}.

ε_w water-filled porosities of a given model cell (*x,y,z*) (equations (D4a)–(D4d)), m^3 m^{-3}.

θ_l water content of the *l*th soil layer (equation (A2)), m^3 m^{-3}.

$\varsigma_{ci,j,z}$ nonstructural carbon of the *i*th plant population, *j*th branch, *z*th aboveground plant organ, product of photosynthesis and nonstructural carbon transfer (equation (C2)), g C m^{-2}.

$\varsigma_{ci,l,z}$ root nonstructural carbon of the *i*th plant population, *l*th soil layer, *z*th root axis, product of photosynthesis and nonstructural carbon transfer (equation (B3)), g C m^{-2}.

$\sigma_{O2GPi,l,z}$ gaseous dispersivity-diffusivity of O_2 in roots, *i*th plant population, *l*th soil layer, *z*th root axis (equation (E1)), m^{-2} h^{-1}.

σ_{O2UR} dispersivity-diffusivity of aqueous O_2 during root uptake (equations (B5b) and ((B5c))), m^2 h^{-1}.

$\sigma\gamma_{AS}$ soil aqueous dispersivity-diffusivity of gas γ at a given model cell (*x,y,z*) in a given horizontal *x*, *y* or vertical *z* direction (equations (D4a)–(D4d)), m^2 h^{-1}.

$\sigma\gamma_{GS}$ soil gaseous dispersivity-diffusivity of gas γ at a given model cell (*x,y,z*) in a given horizontal *x*, *y* or vertical *z* direction (equations (D2a)–(D2c)), m^2 h^{-1}.

$\sigma\gamma_t$ diffusive transfer coefficient (equations (D5) and (E3)), m^2 h^{-1}.

τ_{AS} tortuosity coefficient for aqueous diffusion at a given model cell (*x,y,z*) (equations (D4a)–(D4d)), dimensionless.

$\psi_{t\ i,l,z}$ root turgor potential, *i*th plant population, *l*th soil layer, *z*th root axis (equation (B6), where determines the function $f(\psi_{t\ i,l,z} - \psi_t)$, with ψ_t given in Table 1), MPa.

Abbreviations

DOC dissolved organic carbon, i.e., the products of hydrolysis (only in Appendices A–E), g C m^{-2} h^{-1}.

ER ecosystem respiration, μmol CO_2 m^{-2} s^{-1}.

EC eddy-covariance (technique).

MAE mean absolute error.

RMSD root mean square deviation.

T_l temperature at each soil layer *l* (only in Appendices A–E), °C or °K.

T_S soil temperature, °C or °K.

TDR time domain reflectometry (technique).

WT water table, cm or m.

d Willmott's index of agreement, dimensionless.

γ gas or inorganic solute in gaseous/aqueous phases of soil/plants.

θ soil water content, m^3 m^{-3}.

[69] **Acknowledgments.** Funding was provided by Fluxnet Canada Research Network (FCRN). Computational facilities were provided by Westgrid Canada, University of Bristish Columbia. Data were collected with funding from FCRN through its major sponsors Natural Science and Engineering Council of Canada, Canadian Foundation for Climate and Atmospheric Sciences, and Biocap Canada. Special thanks to Tim Moore and Nigel Roulet, McGill University, Christian Blodau, University of Bayreuth, Germany, Stuart Admiral, Trent University, Yongsheng Feng and Dennis Gignac, University of Alberta.

References

Barnes, B. V., D. R. Zak, S. R. Denton, and S. H. Spurr (1998), *Forest Ecology*, 4th ed., 447 pp., John Wiley, New York.

Blodau, C., and T. R. Moore (2002), Macroporosity affects water movement and pore water sampling in peatland microcosms, *Soil Sci.*, *167* (2), 98–109, doi:10.1097/00010694-200202000-00002.

Blodau, C., N. T. Roulet, T. Heitmann, H. Stewart, J. Beer, P. Lafleur, and T. R. Moore (2007), Belowground carbon turnover in a temperate ombrotrophic bog, *Global Biogeochem. Cycles*, *21*, GB1021, doi:10.1029/2005GB002659.

Bresler, E. (1973), Simultaneous transport of solutes and water under transient unsaturated flow conditions, *Water Resour. Res.*, *9*, 975–986, doi:10.1029/WR009i004p00975.

Bridgham, S. D., C. G. Richardson, E. Maltby, and S. P. Faulkner (1991), Cellulose decay in natural and disturbed peatlands in North Carolina, *J. Environ. Qual.*, *20*, 695–701, doi:10.2134/jeq1991.00472425002000030032x.

Brock, T. D., and M. T. Madigan (1991), *Biology of Microorganisms*, 6th ed., Prentice Hall, Englewood Cliffs, N. J.

Bubier, J. L., P. M. Crill, T. Moore, K. Savage, and R. Varner (1998), Seasonal patterns and controls on net ecosystem CO_2 exchange in a boreal peatland complex, *Global Biogeochem. Cycles*, *12*, 703–714, doi:10.1029/98GB02426.

Bubier, J. L., G. Bhatia, T. R. Moore, N. T. Roulet, and P. M. Lafleur (2003a), Spatial and temporal variability in growing season net ecosystem carbon dioxide exchange at a large peatland in Ontario, Canada, *Ecosystems*, *6*, 353–367.

Bubier, J., P. Crill, A. Mosedale, S. Frolking, and E. Linder (2003b), Peatland responses to varying interannual moisture conditions as measured by automatic CO_2 chambers, *Global Biogeochem. Cycles*, *17*(2), 1066, doi:10.1029/2002GB001946.

Campbell, G. S. (1985), *Soil Physics with BASIC*, Elsevier, Amsterdam.

Davies, J. A. (1981), Models for estimating incoming solar irradiance, *Rep. 81-2*, Can. Clim. Cent., Downsview, Ont., Canada.

Dimitrov, D. D. (2009), Modelling of hydrological and thermal controls on CO_2 exchange at Mer Bleue bog, Ph.D. thesis, Dep. of Renewable Resour., Univ. of Alberta, Edmonton, Alberta, Canada.

Dimitrov, D. D., R. F. Grant, P. M. Lafleur, and E. R. Humphreys (2010a), Modelling subsurface hydrology of Mer Bleue bog, *Soil Sci. Soc. Am. J.*, *74*(2), 680–694, doi:10.2136/sssaj2009.0148.

Dimitrov, D. D., R. F. Grant, P. M. Lafleur, and E. R. Humphreys (2010b), Modelling Peat thermal regime of an ombrotrophic peatland with hummock-hollow microtopography, *Soil Sci. Soc. Am. J.*, *74*(4), 1406–1425, doi:10.2136/sssaj2009.0288.

Falge, E., et al. (2001), Gap filling strategies for defensible annual sums of net ecosystem exchange, *Agric. For. Meteorol.*, *107*, 43–69, doi:10.1016/S0168-1923(00)00225-2.

Frolking, S., N. T. Roulet, T. R. Moore, P. J. H. Richard, M. Lavoie, and S. D. Muller (2001), Modelling northern peatland decomposition and peat accumulation, *Ecosystems*, *4*, 479–498, doi:10.1007/s10021-001-0105-1.

Frolking, S., N. T. Roulet, T. R. Moore, P. M. Lafleur, J. L. Bubier, and P. M. Crill (2002), Modeling seasonal to annual carbon balance of Mer Bleue Bog, Ontario, Canada, *Global Biogeochem. Cycles*, *16*(3), 1030, doi:10.1029/2001GB001457.

Gorham, E. (1991), Northern peatlands: Role in the carbon balance and probable responses to climatic warming, *Ecol. Appl.*, *1*, 182–195, doi:10.2307/1941811.

Grant, R. F. (1989), Test of a simple biochemical model for photosynthesis of maize and soybean leaves, *Agric. For. Meteorol.*, *48*, 59–74, doi:10.1016/0168-1923(89)90007-5.

Grant, R. F. (1993), Simulation model of soil compaction and root growth. I. Model structure, *Plant Soil*, *150*, 1–14, doi:10.1007/BF00779170.

Grant, R. F. (1998a), Simulation in *ecosys* of root growth response to contrasting soil water and nitrogen, *Ecol. Modell.*, *107*, 237–264, doi:10.1016/S0304-3800(97)00221-4.

Grant, R. F. (1998b), Simulation of methanogenesis in the mathematical model *ecosys*, *Soil Biol. Biochem.*, *30*, 883–896, doi:10.1016/S0038-0717(97)00218-6.

Grant, R. F. (2001), A review of the Canadian ecosystem model *ecosys*, in *Modeling Carbon and Nitrogen Dynamics for Soil Management*, edited by M. Shaffer, pp. 173–264, CRC Press, Boca Raton, Fla., doi:10.1201/9781420032635.ch6.

Grant, R. F. (2004), Modelling topographic effects on net ecosystem productivity of boreal black spruce forests, *Tree Physiol.*, *24*, 1–18.

Grant, R. F., and E. Pattey (1999), Mathematical modeling of nitrous oxide emissions from an agricultural field during spring thaw, *Global Biogeochem. Cycles*, *13*, 679–694, doi:10.1029/1998GB900018.

Grant, R. F., and E. Pattey (2003), Modeling variability of N_2O emissions from fertilized agricultural fields, *Soil Biol. Biochem.*, *35*, 225–243, doi:10.1016/S0038-0717(02)00256-0.

Grant, R. F., and P. Rochette (1994), Soil microbial respiration at different temperatures and water potentials: Theory and mathematical modeling, *Soil Sci. Soc. Am. J.*, *58*, 1681–1690, doi:10.2136/sssaj1994.03615995005800060015x.

Grant, R. F., and N. T. Roulet (2002), Methane efflux from boreal wetlands: Theory and testing of the ecosystem model *Ecosys* with chamber and tower flux measurements, *Global Biogeochem. Cycles*, *16*(4), 1054, doi:10.1029/2001GB001702.

Grant, R. F., N. G. Juma, and W. B. McGill (1993a), Simulation of carbon and nitrogen transformations in soil: Mineralization, *Soil Biol. Biochem.*, *25*, 1317–1329, doi:10.1016/0038-0717(93)90046-E.

Grant, R. F., N. G. Juma, and W. B. McGill (1993b), Simulation of carbon and nitrogen transformations in soil: Microbial biomass and metabolic products, *Soil Biol. Biochem.*, *25*, 1331–1338, doi:10.1016/0038-0717(93)90047-F.

Grant, R. F., M. Amrani, D. J. Heaney, R. Wright, and M. Zhang (2004), Mathematical modeling of phosphorus losses from land application of hog and cattle manure, *J. Environ. Qual.*, *33*, 210–233.

Grant, R. F., T. A. Black, E. R. Humphreys, and K. Morgenstern (2007), Changes in net ecosystem productivity with forest age following clear-cutting of a coastal Douglas-fir forest: Testing a mathematical model with eddy covariance measurements along a forest chronosequence, *Tree Physiol.*, *27*, 115–131.

Griffin, D. M. (1972), *Ecology of Soil Fungi*, 193 pp., Syracuse Univ. Press, Syracuse, N. Y.

Griffis, T. J., T. A. Black, D. Gaumont-Guay, G. B. Drewitt, Z. Nesic, A. G. Barr, K. Morgenstern, and N. Kljun (2004), Seasonal variation and partitioning of ecosystem respiration in a southern boreal aspen forest, *Agric. For. Meteorol.*, *125*, 207–223, doi:10.1016/j.agrformet.2004.04.006.

Hogg, E. H., V. J. Lieffers, and R. W. Wein (1992), Potential carbon losses from peat profiles: Effects of temperature, drought cycles and fire, *Ecol. Appl.*, *2*(3), 298–306, doi:10.2307/1941863.

Ju, W., J. M. Chen, T. A. Black, A. G. Barr, H. McCaughey, and N. T. Roulet (2006), Hydrological effects on carbon cycles of Canada's forests and wetlands, *Tellus, Ser. B*, *58*, 16–30.

Klepper, B. (1990), Root growth and water uptake, in *Irrigation of Agricultural Crops*, *Agron. Monogr.*, vol. 30, pp. 281–322, Agron. Soc. of Am., Madison, Wis.

Koike, I., and A. Hattori (1975), Growth yield of a denitrifying bacterium, *Pseudosomonas denitrificans*, under aerobic and denitrifying conditions, *J. Gen. Microbiol.*, *88*, 1–10.

Lafleur, P. M., J. H. McCaughey, D. W. Joiner, P. A. Bartlett, and D. E. Jelinski (1997), Seasonal trends in energy, water, and carbon dioxide fluxes at a northern boreal wetland, *J. Geophys. Res.*, *102*, 29,009–29,020, doi:10.1029/96JD03326.

Lafleur, P. M., N. T. Roulet, J. L. Bubier, S. Frolking, and T. R. Moore (2003), Interannual variability in the peatland-atmosphere carbon dioxide exchange at an ombrotrophic bog, *Global Biogeochem. Cycles*, *17*(2), 1036, doi:10.1029/2002GB001983.

Lafleur, P. M., T. R. Moore, N. T. Roulet, and S. Frolking (2005a), Ecosystem respiration in a cool temperate bog depends on peat temperature but not on water table, *Ecosystems*, *8*, 619–629, doi:10.1007/s10021-003-0131-2.

Lafleur, P. M., R. A. Hember, S. W. Admiral, and N. T. Roulet (2005b), Annual and seasonal variability in evapotranspiration and water table at a shrub-covered bog in southern Ontario, Canada, *Hydrol. Process.*, *19*, 3533–3550, doi:10.1002/hyp.5842.

Letts, M. G., N. T. Roulet, N. T. Comer, M. R. Skarupa, and D. Verseghy (2000), Parameterization of peatland hydraulic properties for the Canadian Land Surface Scheme, *Atmos. Oceans*, *38*, 141–160.

Lizama, H. M., and I. Suzuki (1991), Kinetics of sulfur and pyrite oxidation by *Thiobacillus thiooxidans*. Competitive inhibition by increasing concentrations of cells, *Can. J. Microbiol.*, *37*, 182–187, doi:10.1139/m91-028.

Luxmoore, R. J., L. H. Stolzy, and J. Letey (1970a), Oxygen diffusion in the soil-plant system I. A model, *Agron. J.*, *62*, 317–322, doi:10.2134/agronj1970.00021962006200030003x.

Luxmoore, R. J., L. H. Stolzy, and J. Letey (1970b), Oxygen diffusion in the soil-plant system. II. Respiration rate, permeability and porosity of consecutive excised segments of maize and rice roots, *Agron. J.*, *62*, 322–324, doi:10.2134/agronj1970.00021962006200030004x.

McGill, W. B., H. W. Hunt, R. G. Woodmasee, and J. O. Reuss (1981), Phoenix, a model of the dynamics of carbon and nitrogen in grassland soils, in *Terrestrial Nitrogen Cycles*, *Ecol. Bull.*, *33*, 49–115.

Moore, T. R., and M. Dalva (1993), The influence of temperature and water-table position on carbon dioxide and methane emissions from laboratory columns of peatland soils, *J. Soil Sci.*, *44*, 651–664, doi:10.1111/j.1365-2389.1993.tb02330.x.

Moore, T. R., N. T. Roulet, and J. M. Waddington (1998), Uncertainties in predicting the effect of climatic change on the carbon cycling of Canadian peatlands, *Clim. Change*, *40*, 229–245, doi:10.1023/A:1005408719297.

Moore, T. R., P. M. Lafleur, N. T. Roulet, and S. Frolking (2003), Dependency of ecosystem respiration in a cool temperate bog on peat temperature and water table, *Eos Trans. AGU*, *84*(46), Fall Meet. Suppl., Abstract B22B–04.

Nadelhoffer, K. J., A. E. Giblin, G. R. Shaver, and J. A. Laundre (1991), Effects of temperature and substrate quality on element mineralization in six arctic soils, *Ecology*, *72*(1), 242–253, doi:10.2307/1938918.

Nazaroff, W. W. (1992), Radon transport from soil to air, *Rev. Geophys.*, *30*, 137–160, doi:10.1029/92RG00055.

Oechel, W. C., G. L. Vourlitis, S. J. Hastings, R. P. Ault Jr., and P. Bryant (1998), The effects of water table manipulation and elevated temperature on the net CO_2 flux of wet sedge tundra ecosystems, *Global Change Biol.*, *4*, 77–90, doi:10.1046/j.1365-2486.1998.00110.x.

Orchard, V. A., F. J. Cook, and D. M. Corderoy (1992), Field and laboratory studies on the relationships between respiration and moisture for two soils of contrasting fertility status, *Pedobiologia*, *36*, 21–33.

Powell, G. L. (1980) A comparative evaluation of hourly solar global irradiance models, Ph.D. dissertation, p. 240, Arizona State Univ., Tempe.

Reeve, A. S., D. I. Siegel, and P. H. Glaser (2000), Simulating vertical flow in large peatlands, *J. Hydrol.*, *227*, 207–217, doi:10.1016/S0022-1694(99)00183-3.

Richardson, A. D., et al. (2006), A multi-site analysis of random error in tower-based measurements of carbon and energy fluxes, *Agric. For. Meteorol.*, *136*, 1–18, doi:10.1016/j.agrformet.2006.01.007.

Richardson, D. H. (1981), *The Biology of Mosses*, Blackwell Sci., Oxford, U. K.

Roulet, N. T., P. M. Lafleur, P. J. H. Richard, T. R. Moore, E. R. Humphreys, and J. Bubier (2007), Contemporary carbon balance and late Holocene carbon accumulation in a northern peatland, *Global Change Biol.*, *13*(2), 397–411, doi:10.1111/j.1365-2486.2006.01292.x.

Scanlon, D., and T. R. Moore (2000), Carbon dioxide production from peatland soil profiles: The influence of temperature, oxic/anoxic conditions and substrate, *Soil Sci.*, *165*(2), 153–160, doi:10.1097/00010694-200002000-00006.

Schwarzel, K., M. Renger, R. Sauerbrey, and G. Wessolek (2002), Soil physical characteristics of peat soils, *J. Plant Nutr. Soil Sci.*, *165*, 479–486, doi:10.1002/1522-2624(200208)165:4<479::AID-JPLN479>3.0.CO;2-8.

Shurpali, N. J., S. B. Verma, J. Kim, and T. J. Arkebauer (1995), Carbon dioxide exchange in a peatland ecosystem, *J. Geophys. Res.*, *100*, 14,319–14,326, doi:10.1029/95JD01227.

Silins, U., and R. L. Rothwell (1998), Forest peatland drainage and subsidence affect soil water retention and transport properties in an Alberta peatland, *Soil Sci. Soc. Am. J.*, *62*, 1048–1056, doi:10.2136/sssaj1998.03615995006200040028x.

Silvola, J., and U. Ahlholm (1989), Effects of moisture and temperature on the decomposition of milled and sod peat, in *Proceedings of International Symposium on Peat/Peatland Characteristics and Uses, May 16–20*, Cent. for Environ. Stud., Bemidji State Univ., Bemidji, Minn.

Silvola, J., J. Alm, U. Ahlholm, H. Nykanen, and P. J. Martikainen (1996a), CO_2 fluxes from peat in boreal mires under varying temperature and moisture conditions, *J. Ecol.*, *84*, 219–228, doi:10.2307/2261357.

Silvola, J., J. Alm, U. Ahlholm, H. Nykanen, and P. J. Martikainen (1996b), The contribution of plant roots to CO_2 fluxes from organic soils, *Biol. Fertil. Soils*, *23*, 126–131, doi:10.1007/BF00336052.

Smith, M. R., and R. A. Mah (1980), Acetate as sole carbon and energy source for growth of *Methanosarcina* strain 227, *Appl. Environ. Microbiol.*, *39*, 993–999.

St-Hilaire, F., J. Wu, N. T. Roulet, S. Frolking, P. M. Lafleur, E. R. Humphreys, and V. Arora (2008), McGill Wetland Model: Evaluation of a peatland carbon simulator developed for global assessments, *Biogeosciences Discuss.*, *5*, 1–37, doi:10.5194/bgd-5-1689-2008.

Strack, M., and J. M. Waddington (2007), Response of peatland carbon dioxide and methane fluxes to a water table drawdown experiment, *Global Biogeochem. Cycles*, *21*, GB1007, doi:10.1029/2006GB002715.

Sulman, B. N., A. R. Desai, B. D. Cook, N. Saliendra, and D. S. Mackay (2009), Contrasting carbon dioxide fluxes between a drying shrub wetland in Northern Wisconsin, USA, and nearby forests, *Biogeosciences*, *6*, 1115–1126, doi:10.5194/bg-6-1115-2009.

Updegraff, K., J. Pastor, S. D. Bridgham, and C. A. Johnston (1995), Environmental and substrate controls over carbon and nitrogen mineralization in northern wetlands, *Ecol. Appl.*, *5*, 151–163, doi:10.2307/1942060.

Updegraff, K., S. D. Bridgham, J. Pastor, P. Weisshampel, and C. Harth (2001), Response of CO_2 and CH_4 emissions from peatlands to warming and water table manipulation, *Ecol. Appl.*, *11*, 311–326.

Waddington, J. M., P. A. Rotenberg, and F. J. Warren (2001), Peat CO_2 production in a natural and cutover peatland: Implications for restoration, *Biogeochemistry*, *54*, 115–130, doi:10.1023/A:1010617207537.

Wilhelm, E., R. Battino, and R. J. Wilcock (1977), Low-pressure solubility of gases in liquid water, *Chem. Rev.*, *77*, 219–262, doi:10.1021/cr60306a003.

Willmott, C. J. (1981), On the validation of models, *Phys. Geogr.*, *2*, 184–194.

Willmott, C. J. (1982), Some comments on the evaluation of model performance, *Bull. Am. Meteorol. Soc.*, *63*(11), 1309–1313, doi:10.1175/1520-0477(1982)063<1309:SCOTEO>2.0.CO;2.

Willmott, C. J., and D. E. Wicks (1980), An empirical method for the spatial interpolation of monthly precipitation within California, *Phys. Geogr.*, *1*, 59–73.

Wofford, N. G., P. S. Beaty, and M. J. McInerey (1986), Preparation of cell-free extracts and the enzymes involved in fatty acid metabolism in *Syntrophomonas wolfei*, *J. Bacteriol.*, *167*, 179–185.

Zehnder, A. J., B. A. Huser, T. D. Brock, and K. Wuhrmann (1980), Characterization of an acetate-decarboxylating, non-hydrogen-oxidizing methane bacterium, *Arch. Microbiol.*, *124*, 1–11, doi:10.1007/BF00407022.

D. D. Dimitrov, Northern Forestry Centre, Canadian Forest Service, Edmonton, AB T6H 3S5, Canada.

R. F. Grant, Department of Renewable Resources, University of Alberta, Edmonton, AB T6G 2H1, Canada.

E. R. Humphreys, Department of Geography and Environmental Studies, Carleton University, Ottawa, ON K1S 5B6, Canada.

P. M. Lafleur, Geography Department, Trent University, Peterborough, ON K9J 7B8, Canada.